

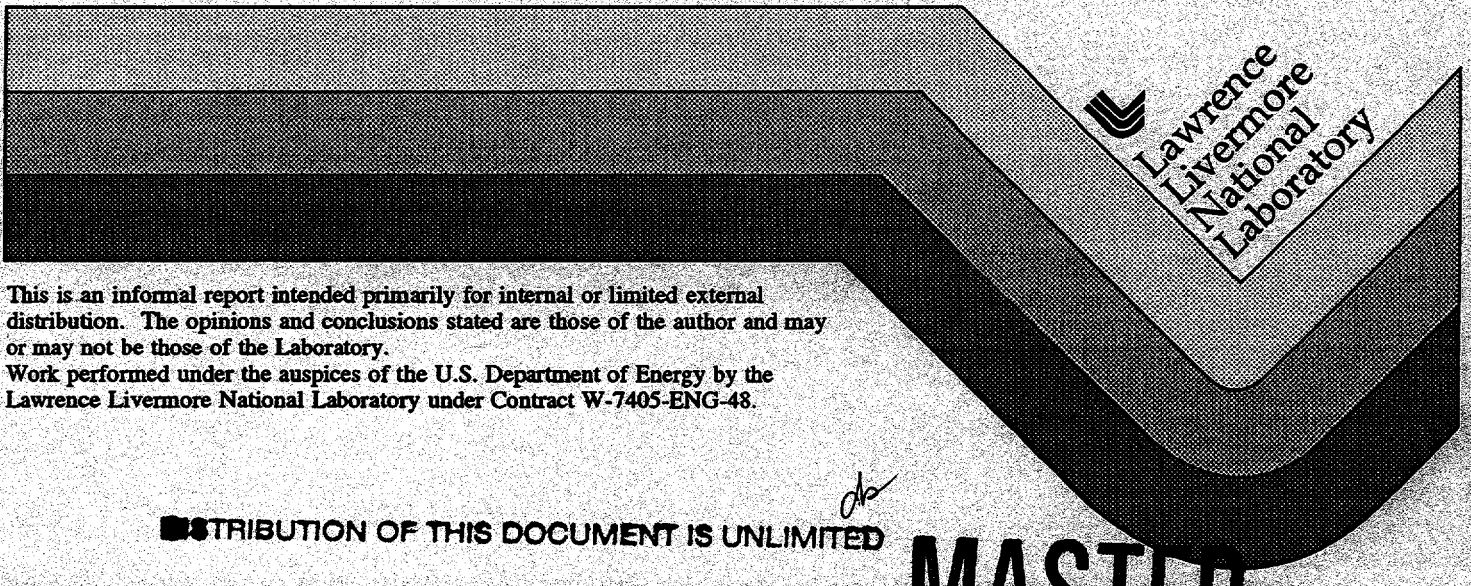
UCRL-ID-125016

FRISCO Containment Data Report

T. Stubbs
R. Heinle

RECEIVED
AUG 16 1996
OSTI

March 1996



This is an informal report intended primarily for internal or limited external distribution. The opinions and conclusions stated are those of the author and may or may not be those of the Laboratory.

Work performed under the auspices of the U.S. Department of Energy by the Lawrence Livermore National Laboratory under Contract W-7405-ENG-48.

DISTRIBUTION OF THIS DOCUMENT IS UNLIMITED

MASTER

DISCLAIMER

This document was prepared as an account of work sponsored by an agency of the United States Government. Neither the United States Government nor the University of California nor any of their employees, makes any warranty, express or implied, or assumes any legal liability or responsibility for the accuracy, completeness, or usefulness of any information, apparatus, product, or process disclosed, or represents that its use would not infringe privately owned rights. Reference herein to any specific commercial products, process, or service by trade name, trademark, manufacturer, or otherwise, does not necessarily constitute or imply its endorsement, recommendation, or favoring by the United States Government or the University of California. The views and opinions of authors expressed herein do not necessarily state or reflect those of the United States Government or the University of California, and shall not be used for advertising or product endorsement purposes.

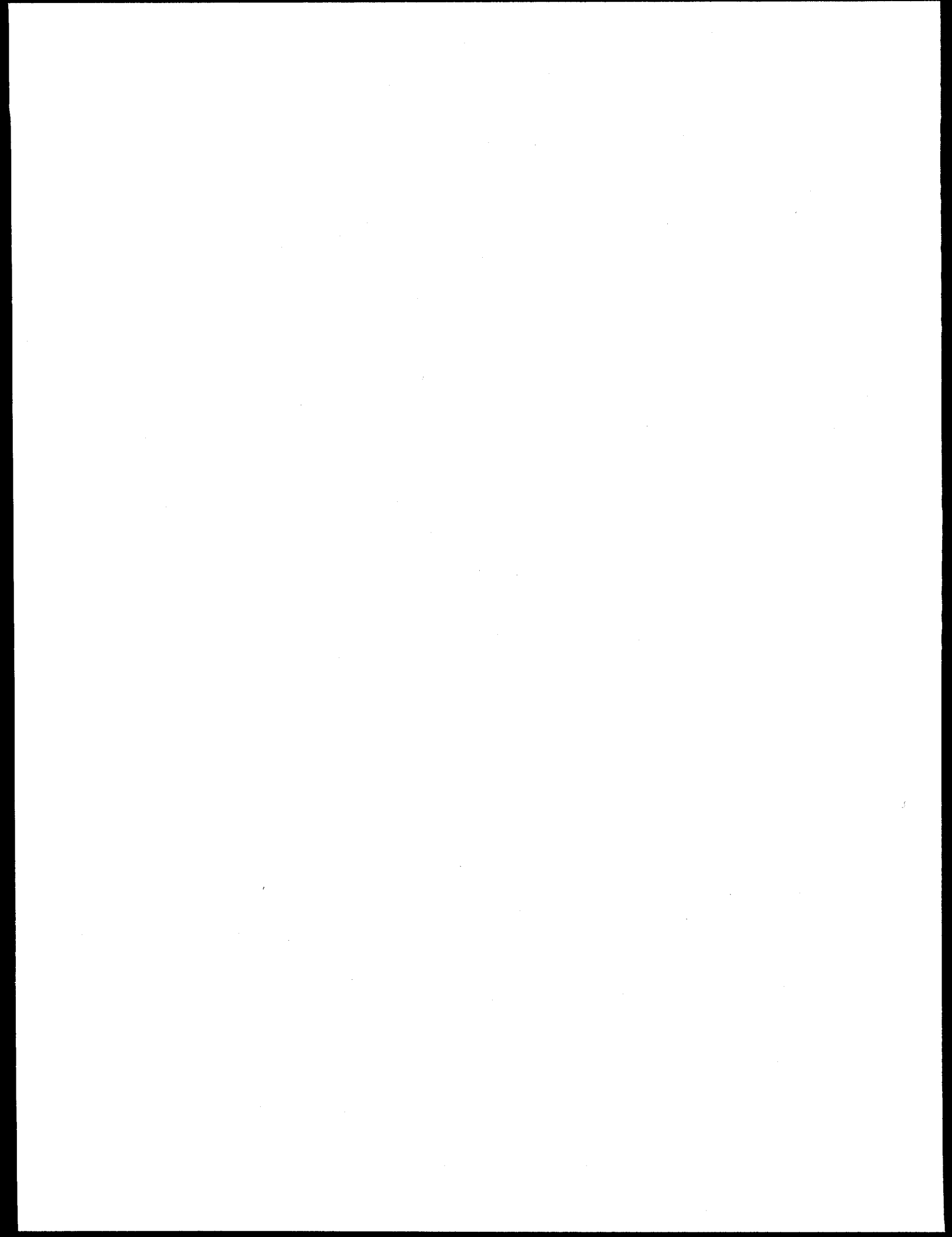
This report has been reproduced
directly from the best available copy.

Available to DOE and DOE contractors from the
Office of Scientific and Technical Information
P.O. Box 62, Oak Ridge, TN 37831
Prices available from (615) 576-8401, FTS 626-8401

Available to the public from the
National Technical Information Service
U.S. Department of Commerce
5285 Port Royal Road
Springfield, VA 22161

DISCLAIMER

**Portions of this document may be illegible
in electronic image products. Images are
produced from the best available original
document.**



FRISCO Instrumentation Summary

Instrumentation	Fielded on this Event	Data Return	Present in this Report
<u>Plug Emplacement</u>	yes	yes	yes(a)
<u>Radiation</u>	yes	yes	yes
<u>Pressure</u>			
Stemming	yes	yes	yes
Challenge	no	-	-
Cavity	no	-	-
Atmospheric	no	-	-
<u>Motion</u>			
Free Field	no	-	-
Surface	yes	yes	yes
Plug	yes	yes	yes
Stemming	no	-	-
Surface Casing	yes	yes	yes
Emplacement Pipe	yes	yes	yes
<u>Hydroyield</u> (b)	yes	yes	no
<u>Collapse</u> (c)	yes	no	-
<u>Stress</u>	no	-	-
<u>Strain</u> (d)	yes	yes	no
<u>Other Measurements</u> (e)	yes	yes	yes

- (a) Description only.
- (b) CORTEX and/or SLIFER in emplacement hole.
- (c) EXCOR or CLIPER in emplacement hole.
- (d) Strain load on emplacement pipe.
- (e) Geophone array and pressure and temperature in the device canister.

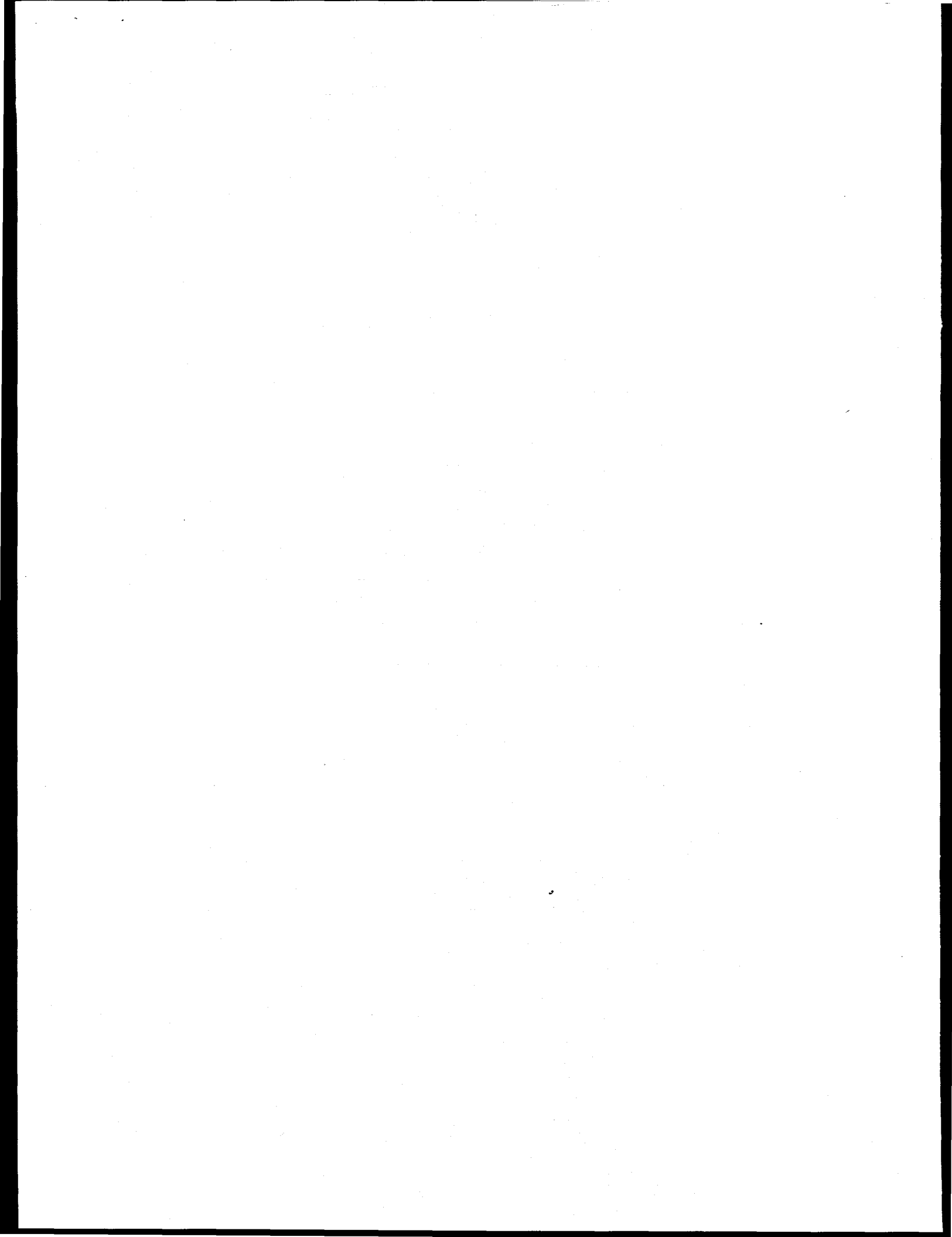
Event Personnel

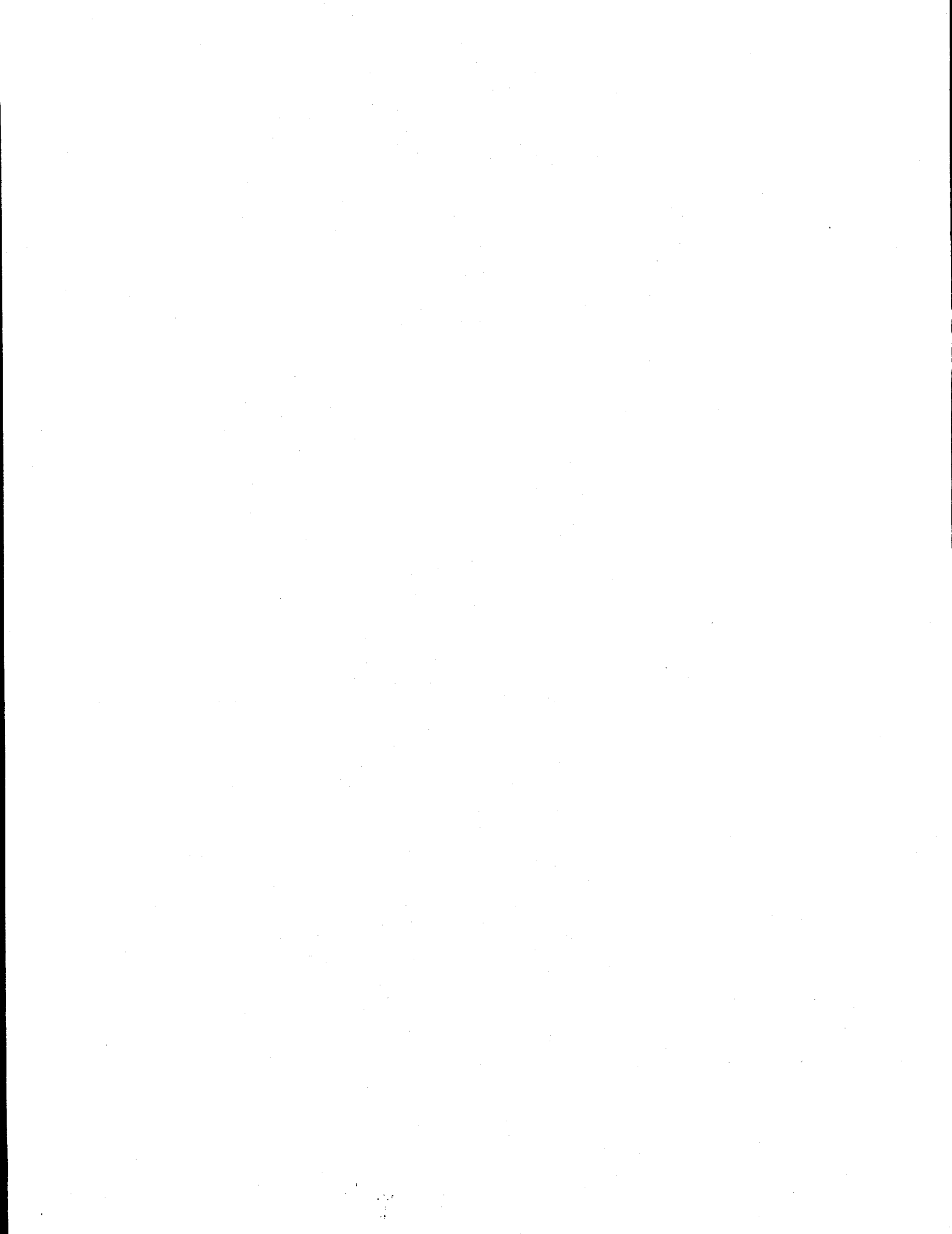
Containment Physics

B. Hudson	LLNL
V. Wheeler	LLNL
J. Kalinowski	EG&G/AVO
T. Stubbs	EG&G/AVO

Instrumentation

C. Cordill	LLNL
M. Hatch	EG&G/AVO
L. Davies	EG&G/NVO
L. Farthing	EG&G/NVO





1. Event Description

1.1 Site

The FRISCO event was detonated in hole U8m of the Nevada Test Site as indicated in figure 1.1. The FRISCO device had a depth-of-burial (DOB) of 452 m in the Fraction Tuff of area 8, about 160 m above the Paleozoic formation and 100 m above the standing water level, as shown in the geologic cross-sections of figures 1.2 and 1.3⁽¹⁾. Stemming of the 2.44 m diameter emplacement hole followed the plan shown in figure 1.4. A log of the stemming operations was maintained by Holmes & Narver⁽²⁾.

Detonation time was 10:00 PDT on September 23, 1982, and collapse progressed to the surface at about 0.5 hour after detonation. The resulting crater had a mean radius of 69.5 m and a maximum depth of 5.3 m

No radiation arrivals were detected above ground and the FRISCO containment was considered successful.

1.2 Instrumentation

Figure 1.5 is a schematic layout of the instrumentation designed to monitor the emplacement procedures and stemming performance of the FRISCO event.

Pressure and radiation were monitored at only one station; in the coarse stemming just below the top plug.

Gas pressure and temperature measurements were attempted on a pinex pipe within the device canister. These quantities were monitored on the pinex collar and on the pinex hat. Strain (load) on the emplacement pipe was monitored during emplacement and noted from time to time in the stemming log⁽²⁾.

Vertical motion of the stemming plug, the surface casing, and the emplacement pipe as well as the motion of the ground surface, 15.42 m from SGZ was monitored. Relative motion of the surface casing and the top plug was derived from these measurements. Displacement transducers (reel-type extensometers) were mounted between the surface casing and the backfill above the top plug and also between the surface casing and the emplacement pipe to obtain a direct measure of this relative motion.

Displacement transducers were also installed to detect the displacement of stemming (slump) below each of the three plugs during stemming operations. Output from these devices was monitored during and after the event, yielding some information on the collapse.

Data from each of the above instruments were transmitted to the recording trailer by an analog system and recorded on magnetic tape.

One CLIPER/CORRTEX sensor attached to the device canister and emplacement pipe was fielded to estimate device yield and to monitor cavity collapse and chimney formation. Results of the yield measurement are reported elsewhere⁽³⁾.

A history of the fielding operations of the instrumentation is outlined in reference 4. Details of the instrumentation are given in reference 5.

1.3. Emplacement

All three of the stemming plugs above the FRISCO event were composed of rigid coal-tar epoxy (LAE 59, denoted CTE) The top plug was about 7.6 m thick while the lower two lower plugs were about 2.3 m thick. A soft (about 2.2 m thick) layer of coal-tar and aggregate (LAE 59MY, denoted CTA) was poured on each of the three plugs to act as a gas seal. The emplacement pipe was "greased" with hydroseal in the regions of the plugs to allow the pipe to move freely through the plugs. Stemming between the plugs consisted of layers of fines and coarse gravel. The top of the hole (above the top plug) was filled with ground surface derived backfill and the inside of the emplacement pipe was grouted for its full length. See figure 1.4.

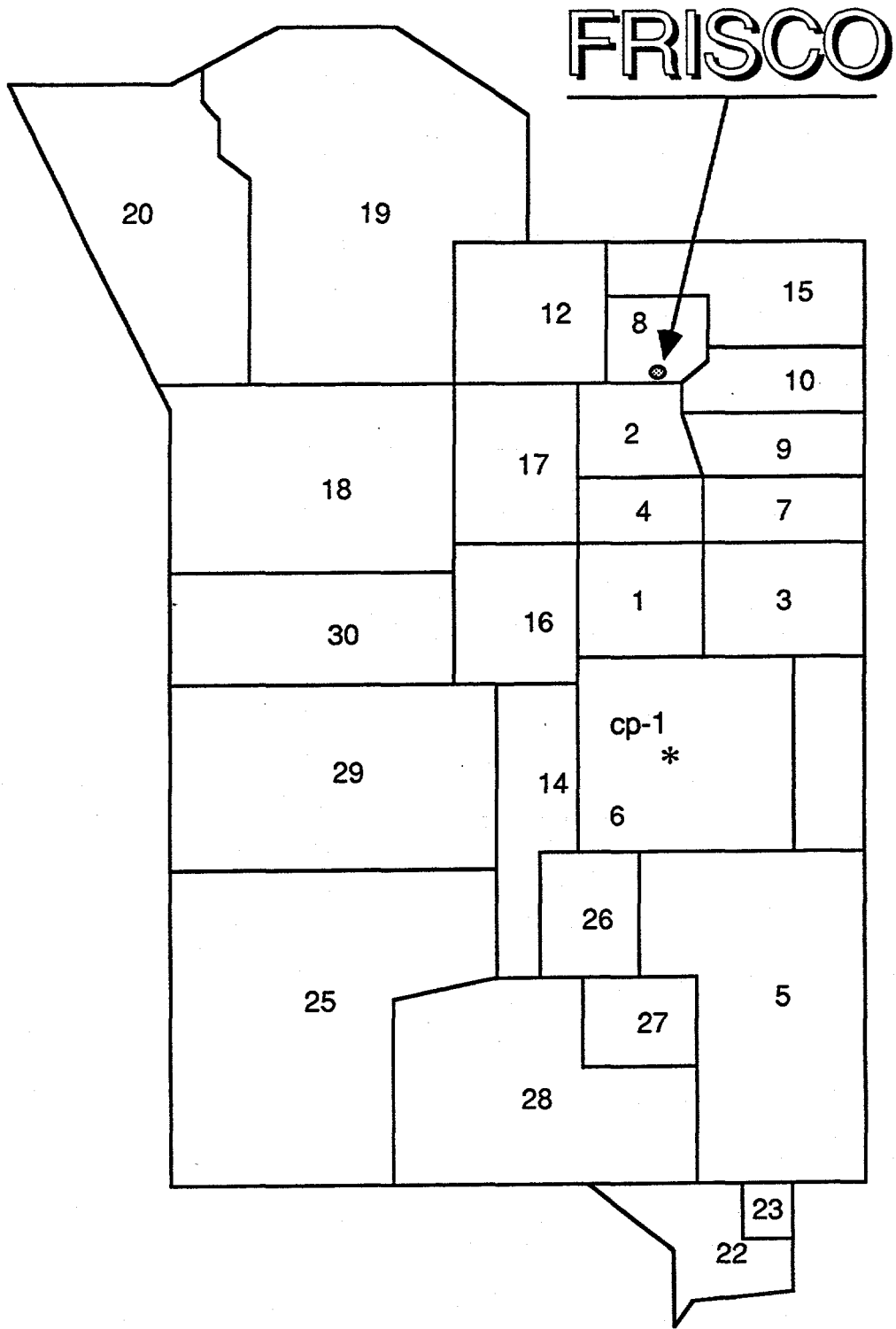


Figure 1.1 Map of the Nevada Test Site indicating the location of hole U8m.

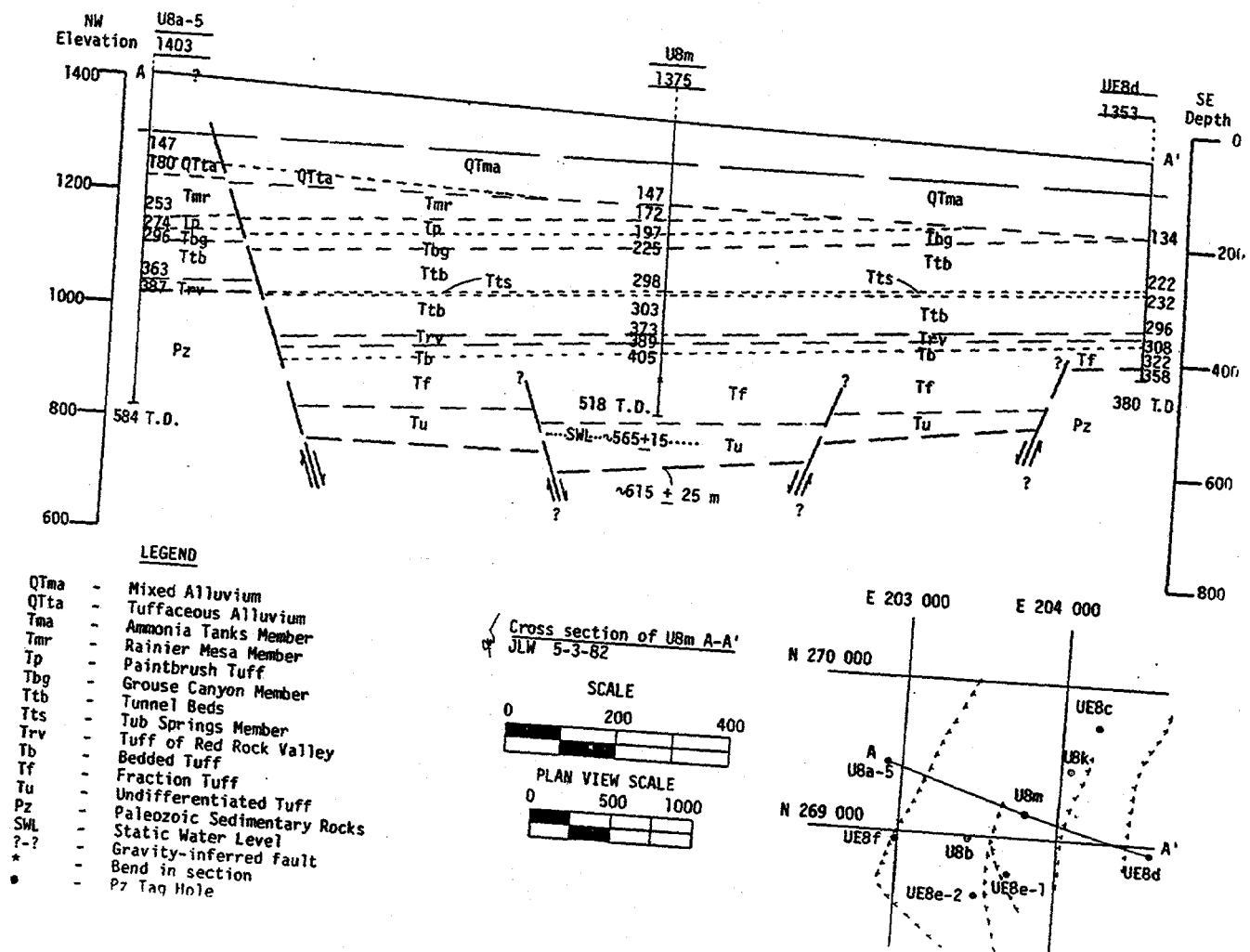


Figure 1.2 East-West geologic cross section through hole U8m.

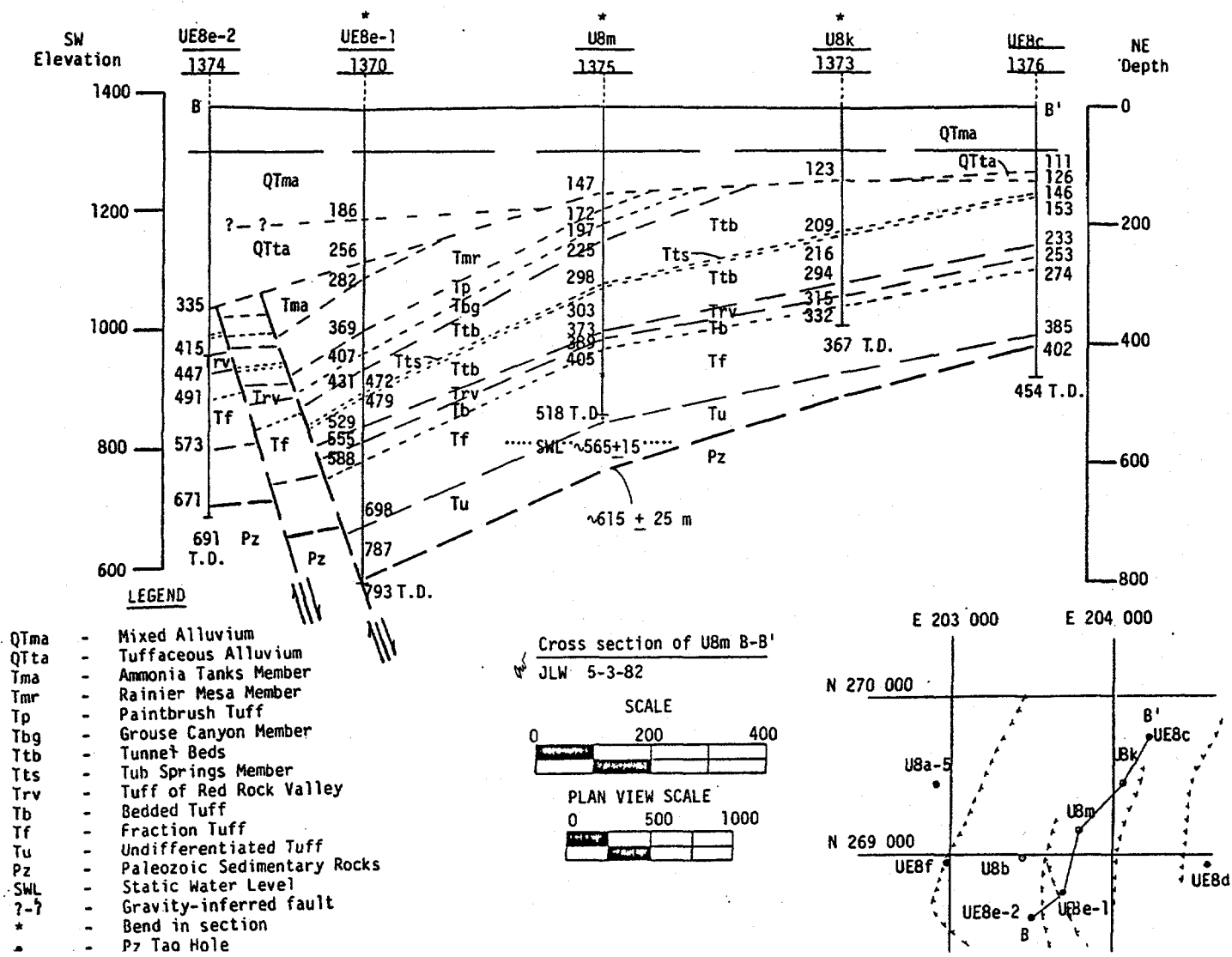
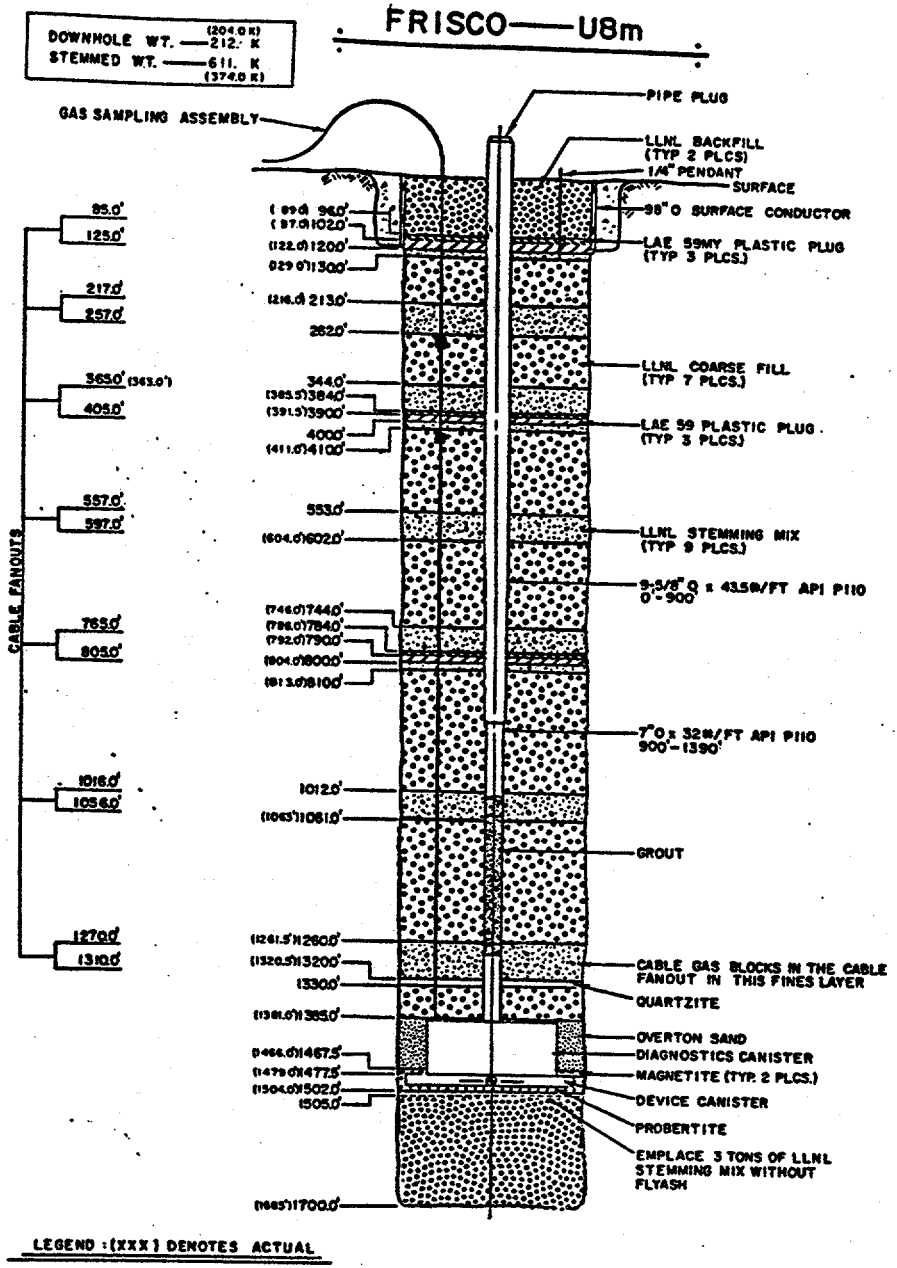


Figure 1.3 North-South geologic cross section through hole U8m.



HOLMES & HARVER INC

Figure 1.4 As-built stemming plan for the event FRISCO in Hole U8m.

2. Stemming Performance

2.1 Radiation and Pressure

Pressure and radiation were monitored on the FRISCO at the one station (31) below the top plug as shown in figure 1.5. These measurements are shown in figures 2.1 and indicate that no radiation reached this elevation and only a slight, brief explosion-induced pressure drop at detonation time was seen.

The radiation data are consistent with satisfactory containment.

2.2 Motion

Explosion-induced histories of the motion measured on the FRISCO event are shown in figures 2.2–2.6. Characteristics of the associated motion and transducers are given in tables 2.2–2.4.

Relative motion of the surface casing and top plug is shown in figure 2.7. Here the difference between the derived displacement of station 62 (the surface casing) and station 26 (the top plug) is shown. During the first eight seconds after detonation there is almost no separation between these elements: it is zero, to the accuracy of the measurements. Also shown is the extensometer data from station 32 (between the surface casing and an anchor in the backfill within the casing). If the top plug remains attached to the casing, the 0.72 m of extension observed (initial extension is 0.28 m) may be attributable to compaction of the stemming material above the plug. Considering the full depth of stemming between the anchor of station 32 and the top of the top plug (26.95 m) this suggests a final linear compaction of 2.6% at 8 s after detonation.

Figure 2.8 shows the relative vertical displacement between the emplacement pipe (station 63) and the surface casing (station 62). Also shown is the derived vertical separation between these two elements as derived from the extensometer between them (station 33). Initially, the connection of the transducer was on the emplacement pipe vertically 1.12 m above the attachment to the surface casing and 0.70 m horizontally apart from it. It was assumed that all motion was vertical. The wave form for station 33 was set to be on the baseline before the detonation. A close agreement between the extensometer history and that of the difference of the displacement of stations 63 and 62 is observed.

Each of the plugs was instrumented with a pair of extensometers to sense stemming slump during and after stemming and the system was recorded during and after the detonation. Figures 2.9 - 2.11 show the wave forms of each of these transducers. The sand anchors were held in position by explosive bolts until stemming covered them and then the bolts were fired, releasing the anchors for measurement. When the bolts on the anchors of stations 84 and 85 (middle plug) were fired the anchors fell about 1 m, almost the full extension of the transducer. This rendered these stations nearly unusable. Each of the extensometers at the bottom and top plugs had an initial extension of between 15 and 20 cm and underwent an explosion-induced extension of about 3 cm (figures 2.9 and 2.11).

2.3 Collapse phenomena

Collapse-induced histories of the motion measured on the FRISCO event are shown in figures 2.12–2.15. Collapse reached the ground surface at 1836 s after detonation with slap-down occurring about 1.7 s later. The only down-hole collapse indications were from the extensometer transducers, as seen in figures 2.9 - 2.11. Time of the progression of the collapse front as a function of depth is given in the following table.

Table 2.1 Collapse Progression

Station	Depth (m)	Collapse (s)
81 & 82	245.7	1832.6
84 & 85	122.5	1836.2*
87 & 88	38.6	1837.0
32	0	1837.0

* These stations probably malfunctioned.

The wave form of the relative displacement between the surface casing and top plug during collapse is shown in figure 2.7 along with the extensometer reading between the surface casing and the stemming at the top of the hole. If the difference between the displacements of stations 62 and 26 are correct, the top plug was driven into the surface casing by about 35 cm by the slap-down of collapse. The extensometer increases by about 70 cm leading to a final compression of the backfill stemming above the top plug of about 6.6 %. Close agreement between the extensometer history and that of the difference of the displacement of stations 63 and 62 during collapse is also shown in figure 2.8. Figures 2.9 - 2.11 show the behavior of the plug-associated extensometers during collapse. Again, since the transducers associated with the middle plug were mounted at their maximum extension, it is expected that only the collapse time is available from them.

Note the two-stage collapse experienced by the emplacement pipe (figure 2.14). The first drop occurs at about 1835.2 s, midway between the times the collapse front passes the deepest plug and the middle plug (see table 2.1). The pipe then falls slowly until the surface collapse terminates with slap-down at about 1837.2 s.

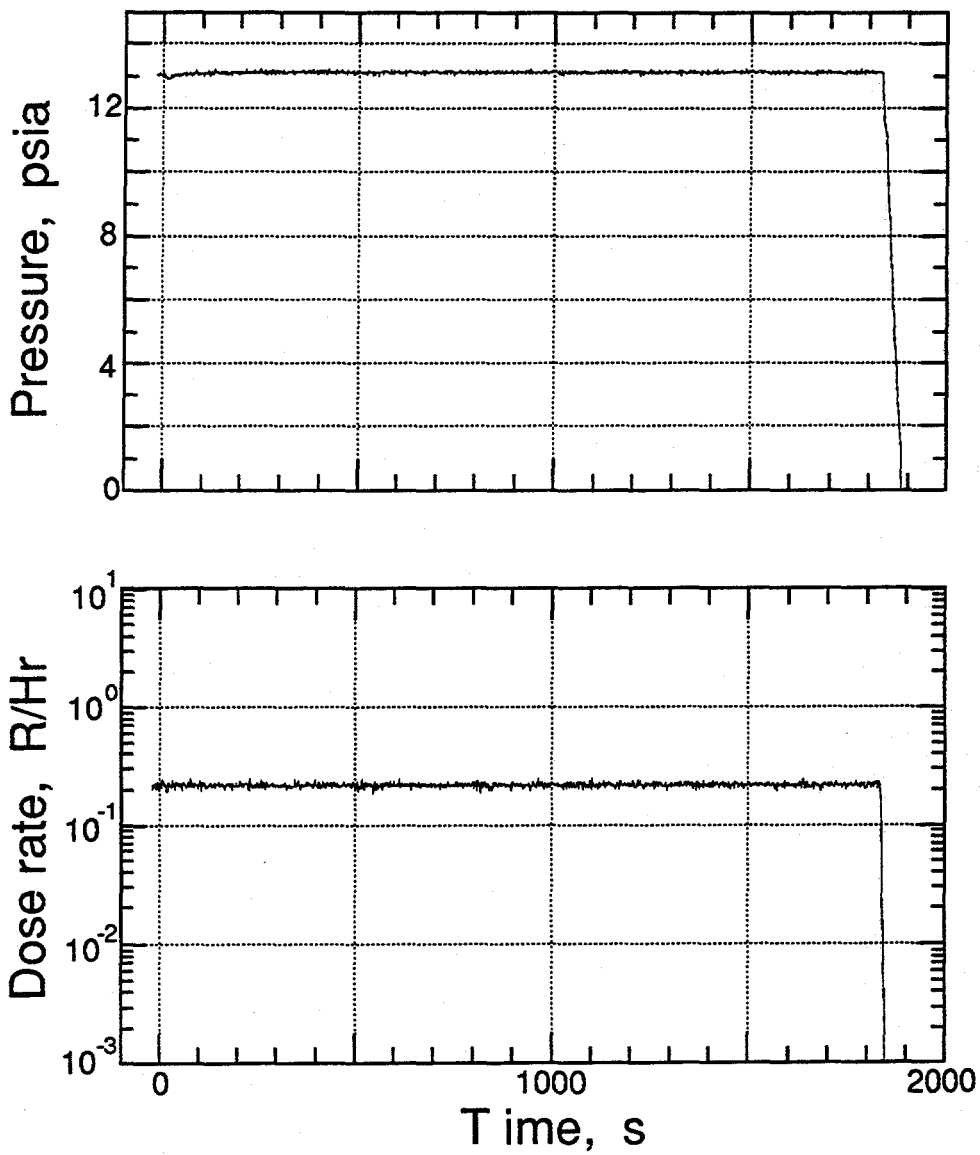
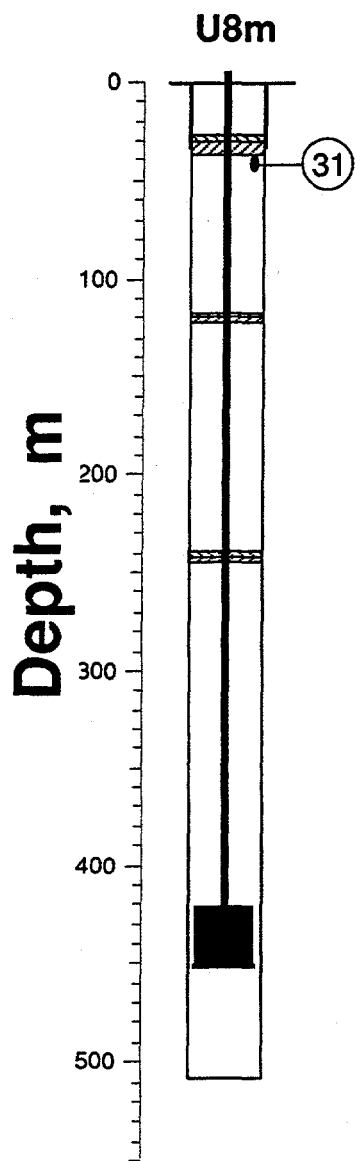


Figure 2.1 Pressure and radiation measured in the coarse stemming below the top plug (station 31 at a depth of 42.7 m).

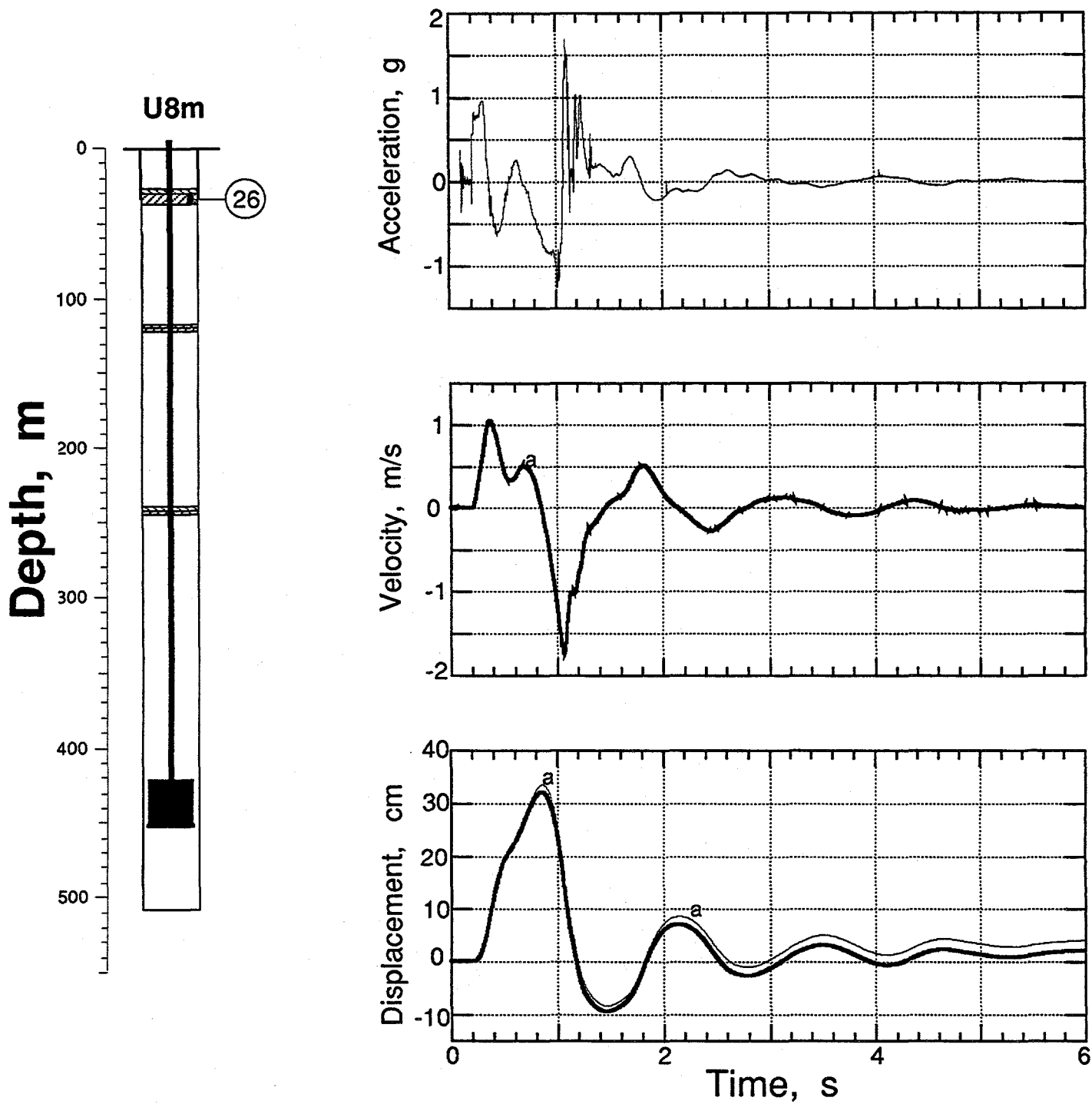


Figure 2.2 Explosion-induced vertical motion of the top plug (station 26 at a depth of 34.5 m) The traces annotated with "a" are derived from the acceleration while the velocimeter-derived signals are shown as heavy traces.

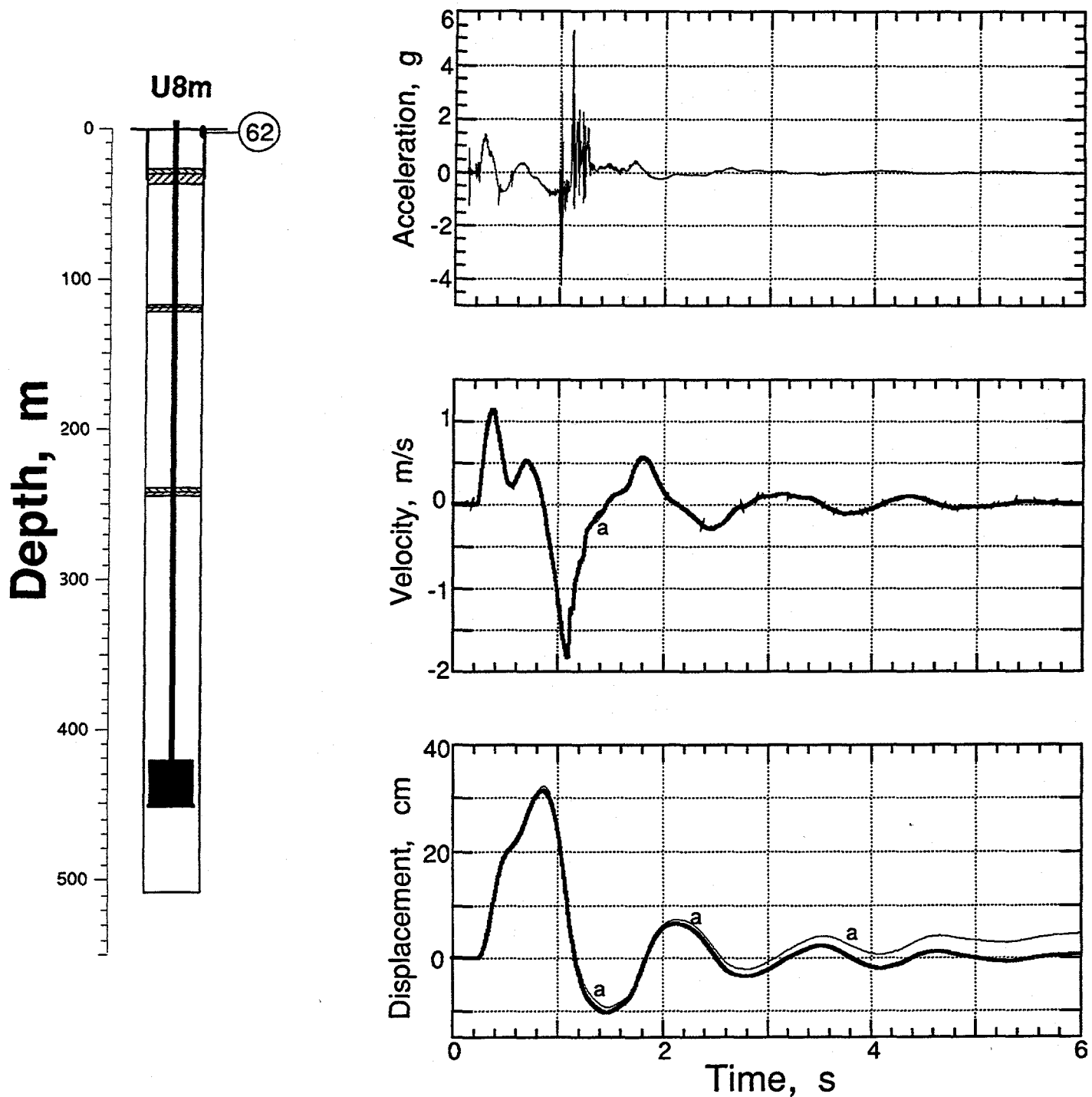


Figure 2.3 Explosion-induced vertical motion of the surface casing (station 62) The traces annotated with "a" are derived from the acceleration while the velocimeter-derived signals are shown as heavy traces.

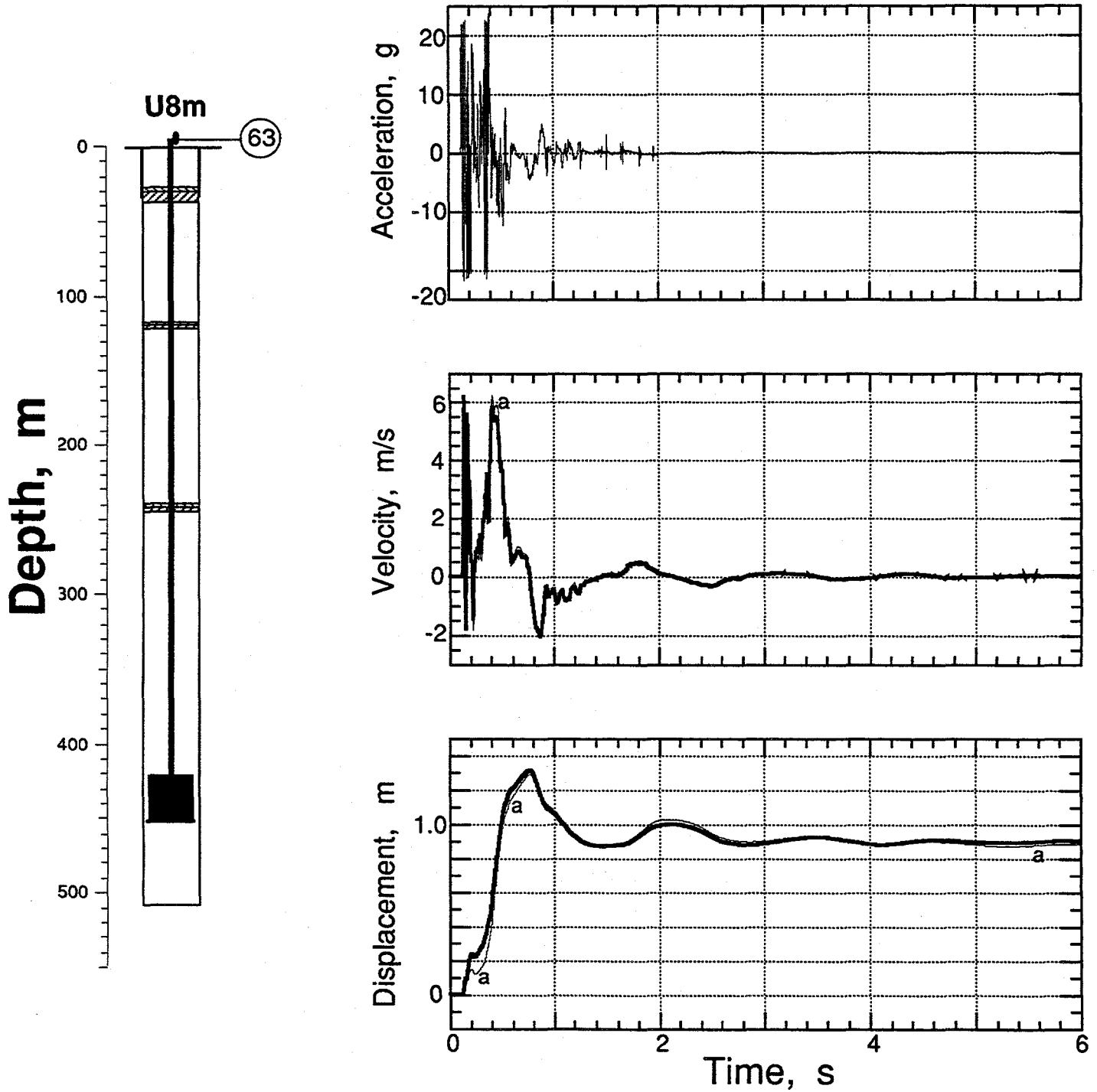


Figure 2.4 Explosion-induced vertical motion of the emplacement pipe (station 63) The traces annotated with "a" are derived from the acceleration while the velocimeter-derived signals are shown as heavy traces.

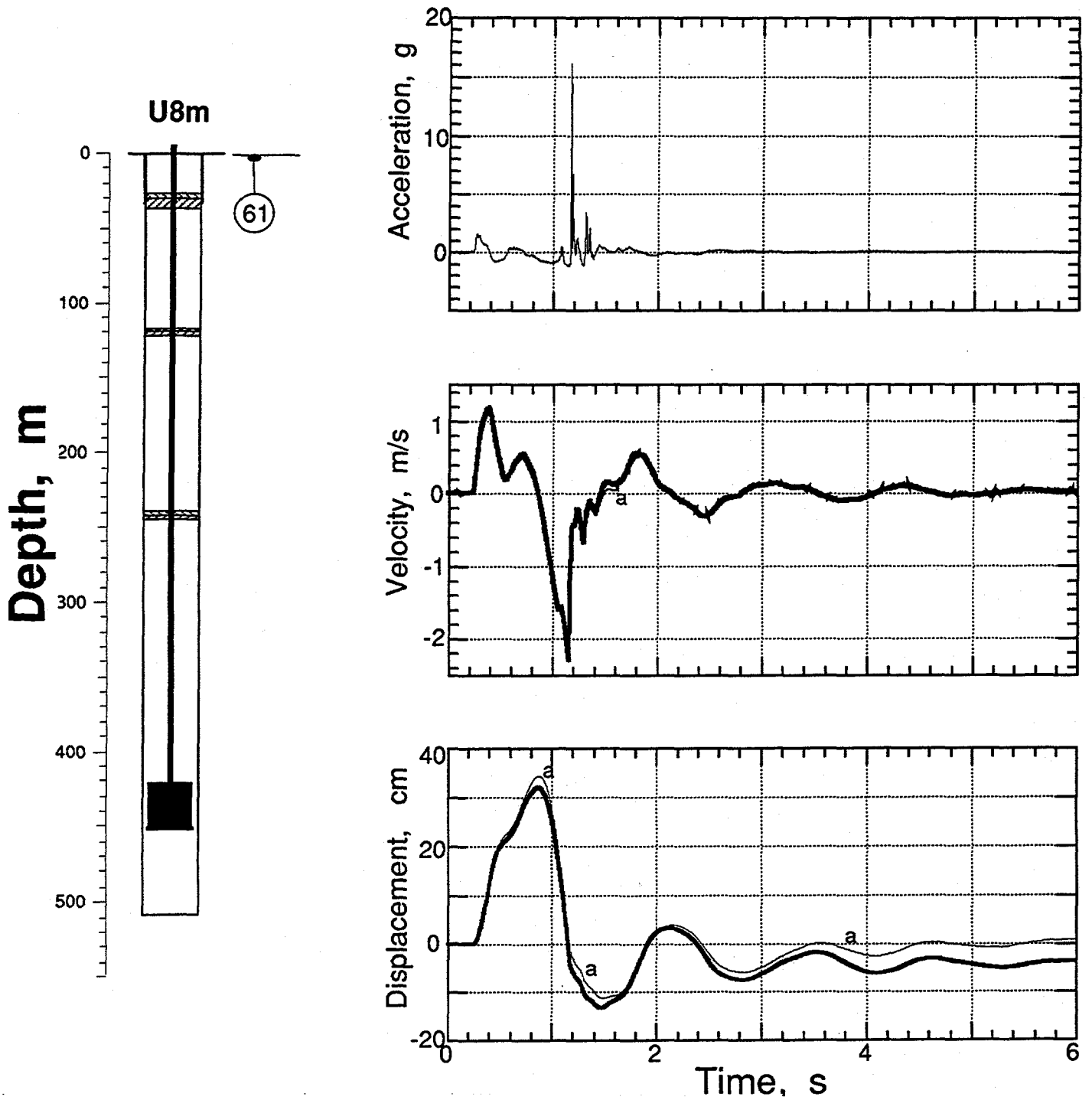


Figure 2.5 Explosion-induced vertical motion of the ground surface, 15.24 from SGZ (station 61 at a depth of 0.9 m) The traces annotated with "a" are derived from the acceleration while the velocimeter-derived signals are shown as heavy traces.

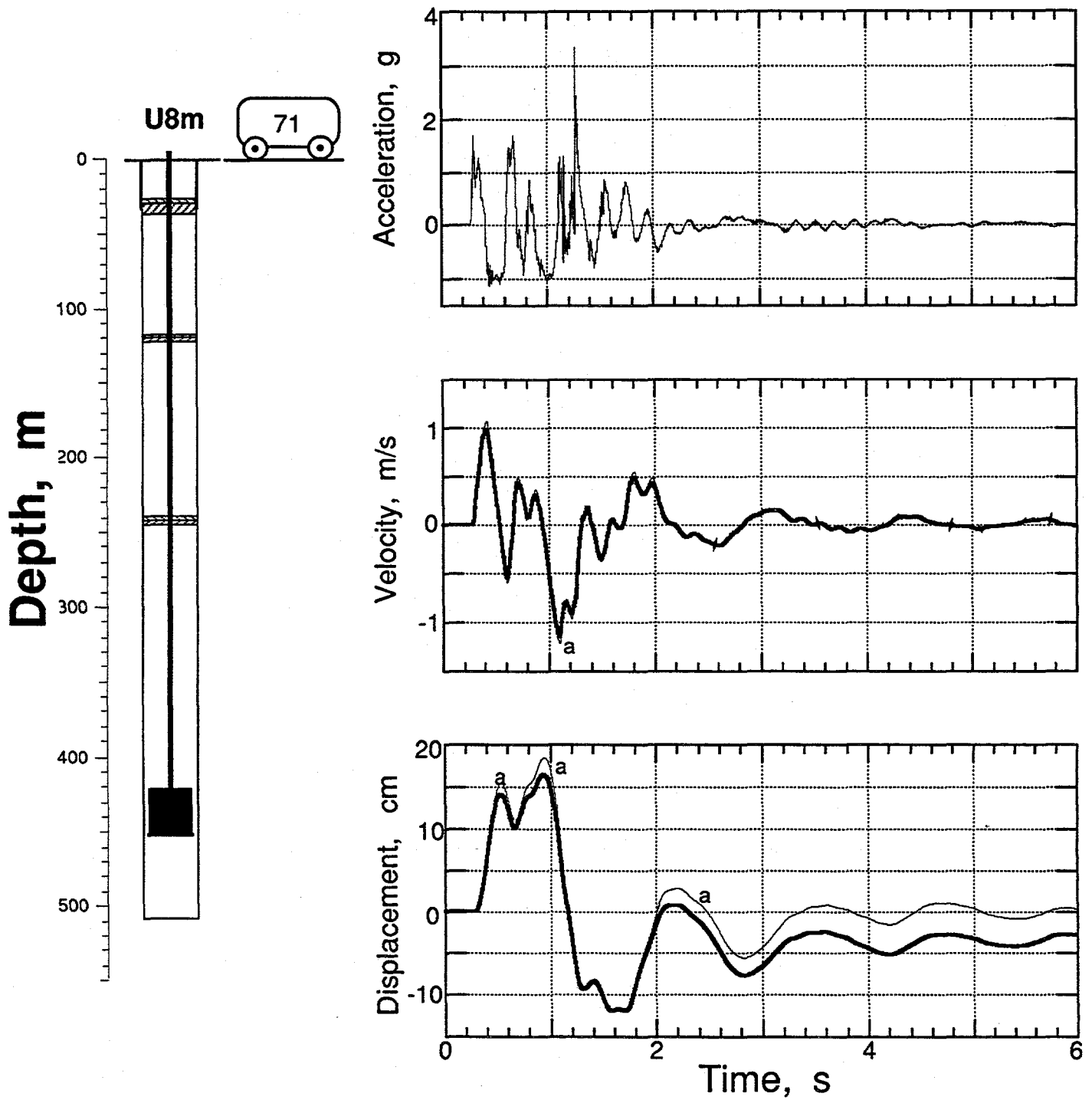


Figure 2.6 Explosion-induced vertical motion of the instrumentation trailer (station 71) The traces annotated with "a" are derived from the acceleration while the velocimeter-derived signals are shown as heavy traces.

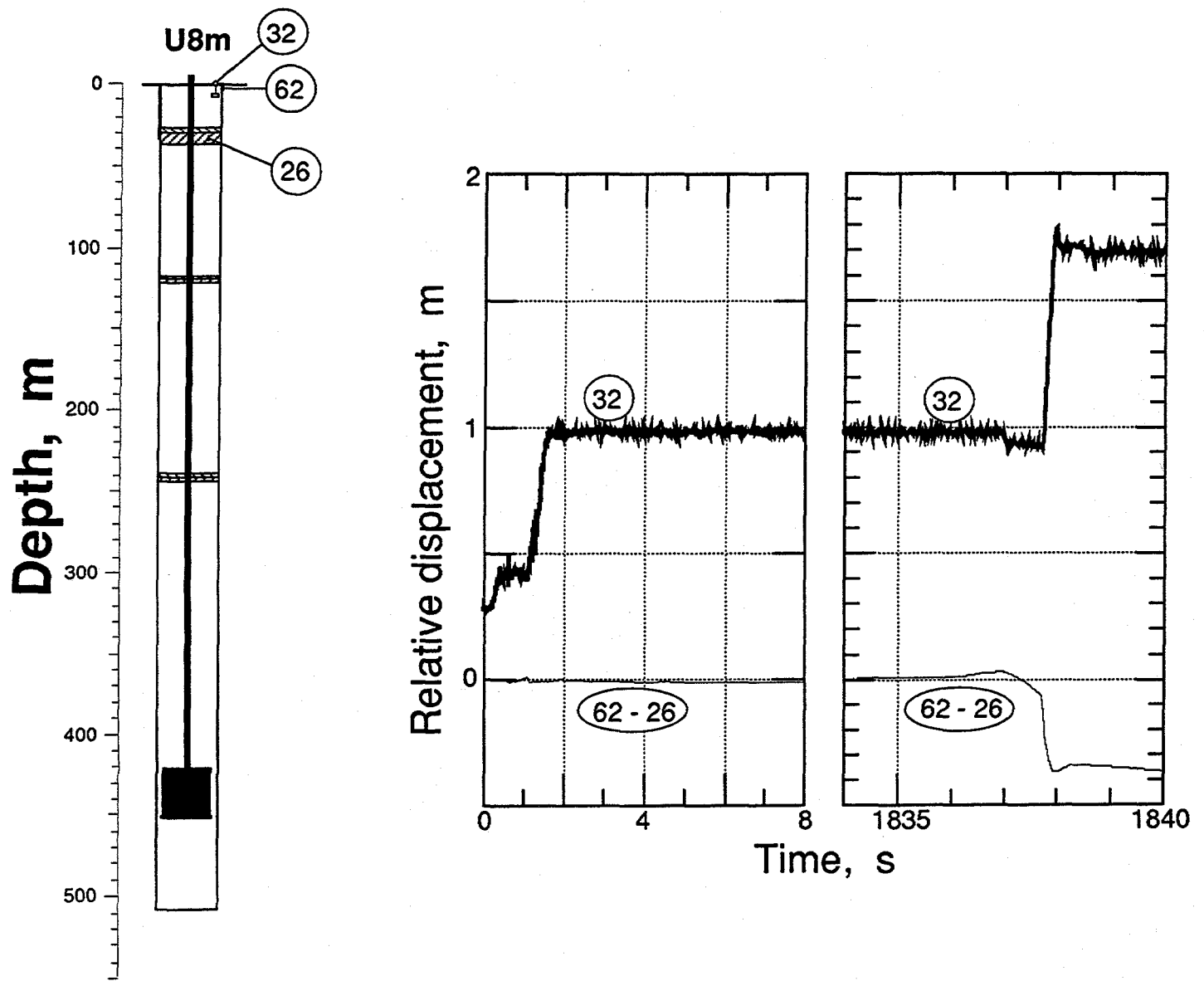


Figure 2.7 Relative vertical motion between surface casing and top plug (difference between displacement of stations 62 and 26) plotted with extensometer of station 32 (between surface casing and an anchor in the backfill).

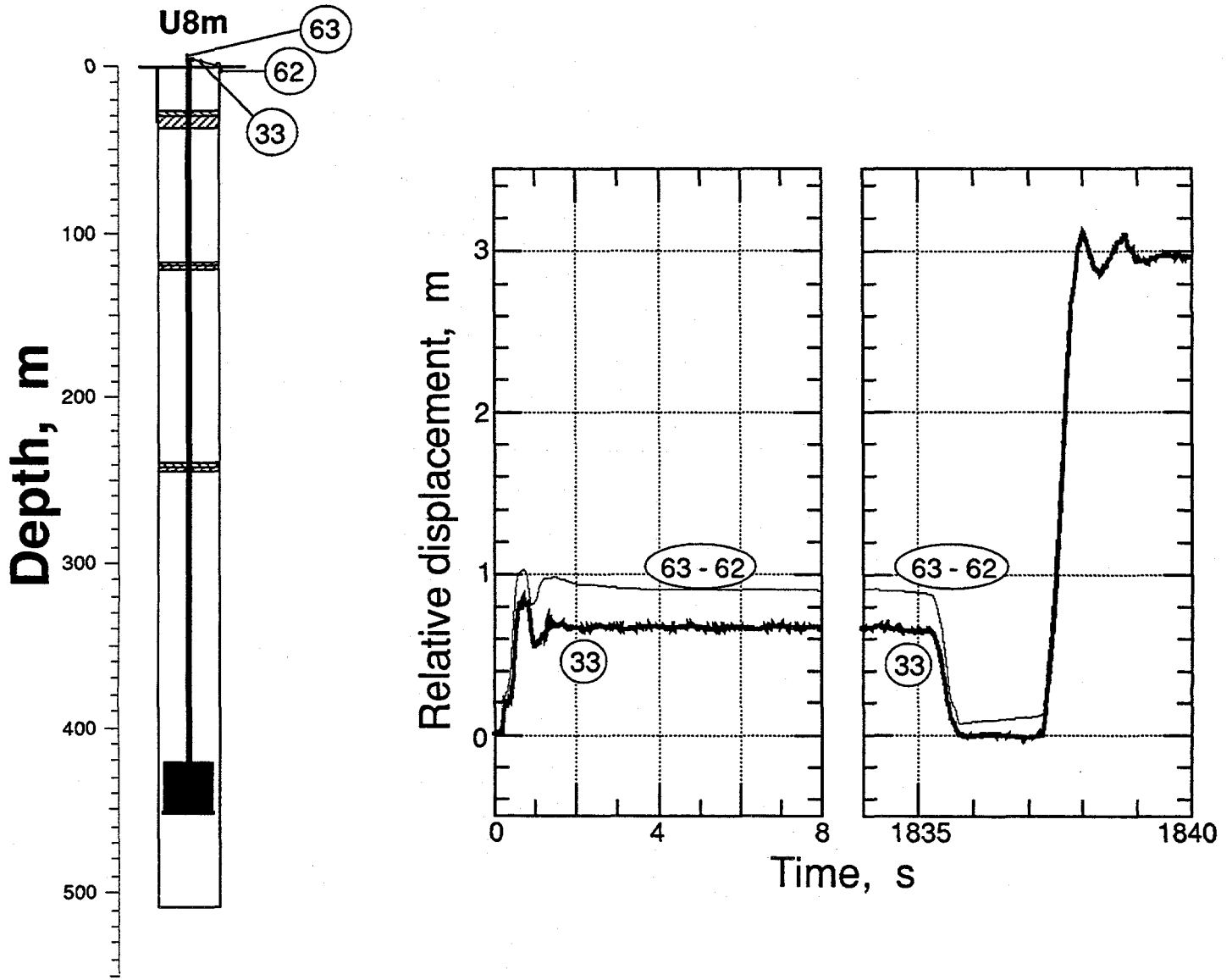


Figure 2.8 Relative vertical motion between surface casing and emplacement pipe (difference between displacement of stations 63 and 62) plotted with extensometer of station 33 (between surface casing and emplacement pipe).

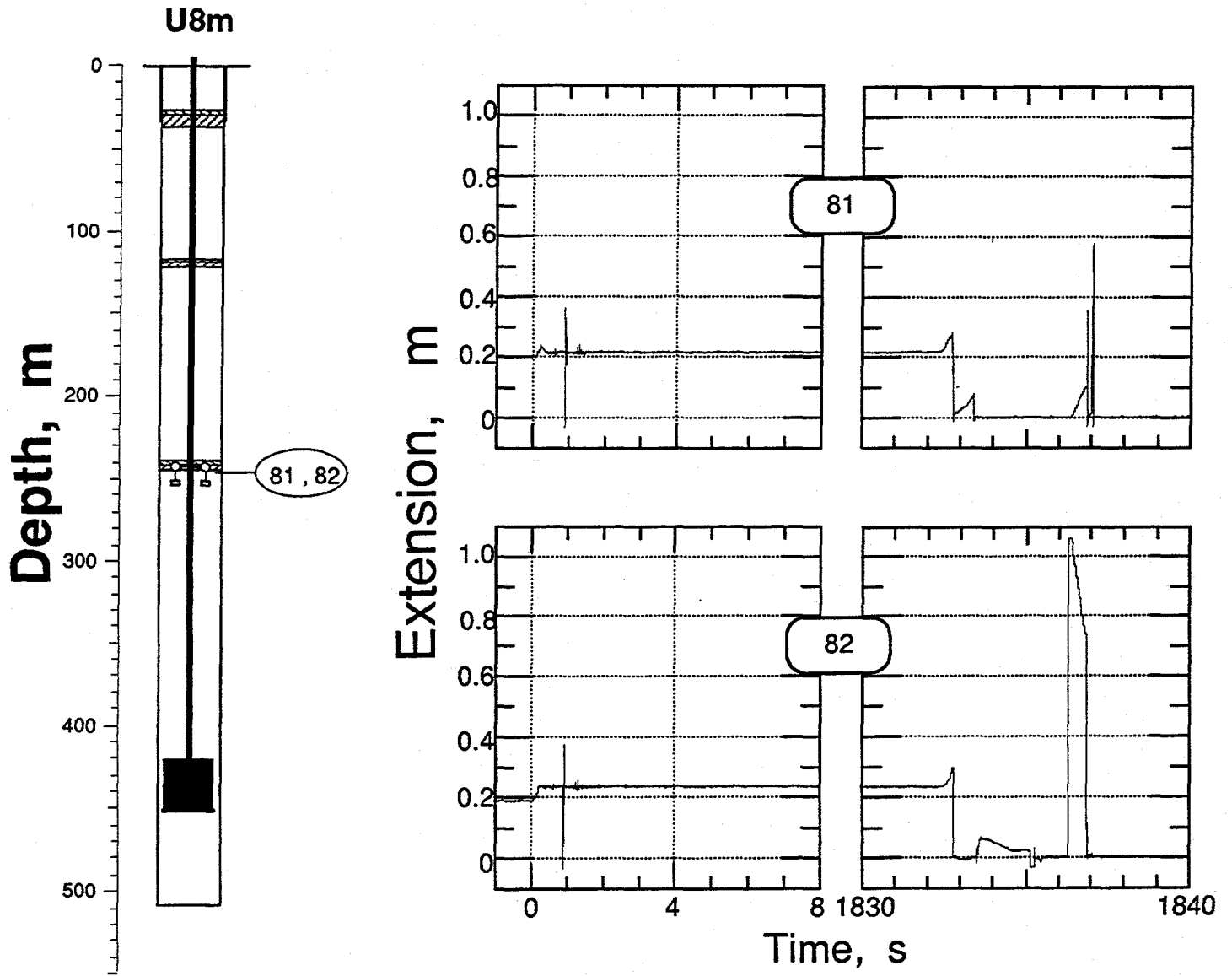


Figure 2.9 Extensometer readings from stations 81 and 82, mounted between bottom plug and underlying stemming.

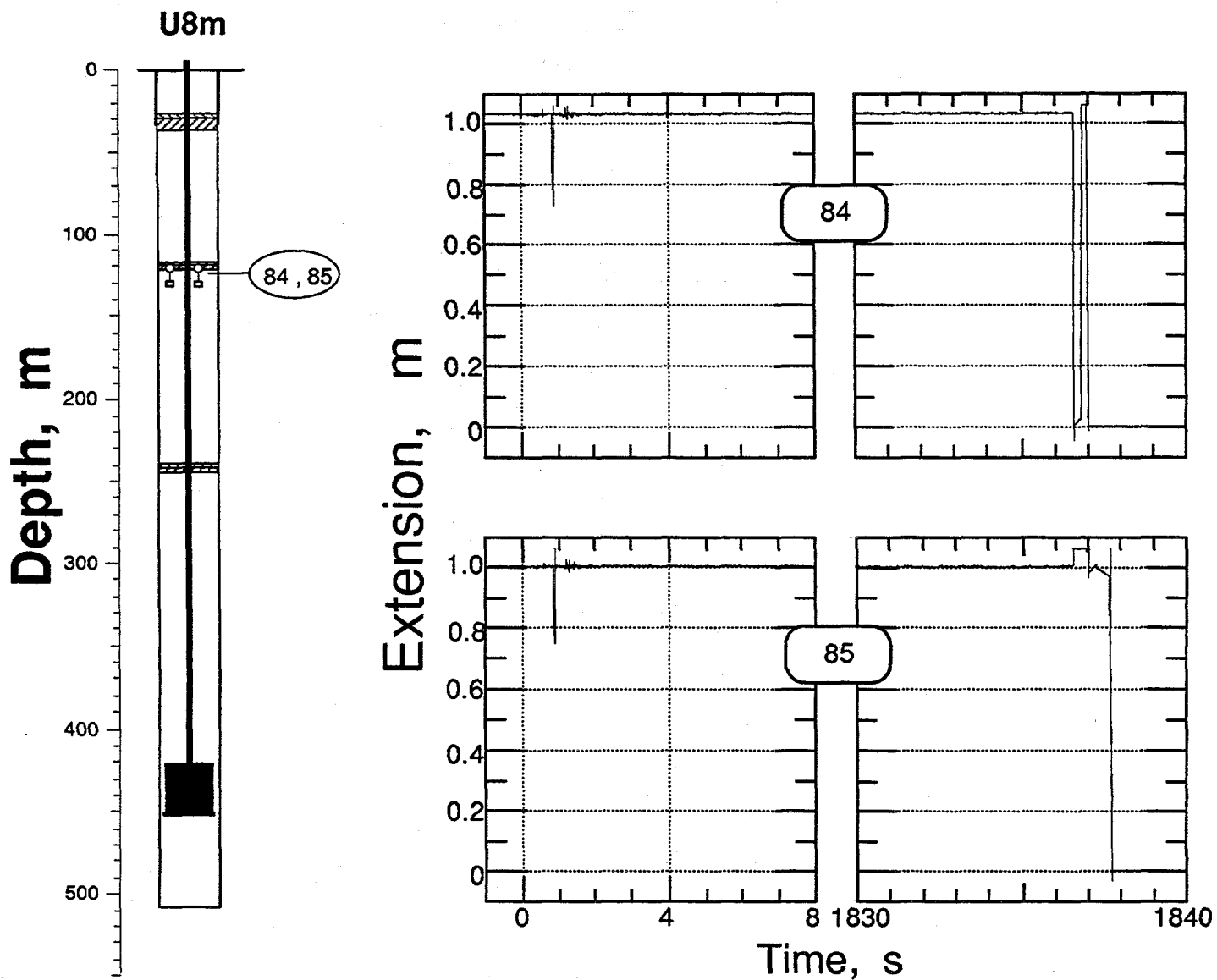


Figure 2.10 Extensometer readings from stations 84 and 85, mounted middle bottom plug and underlying stemming. These gauges seem to have malfunctioned.

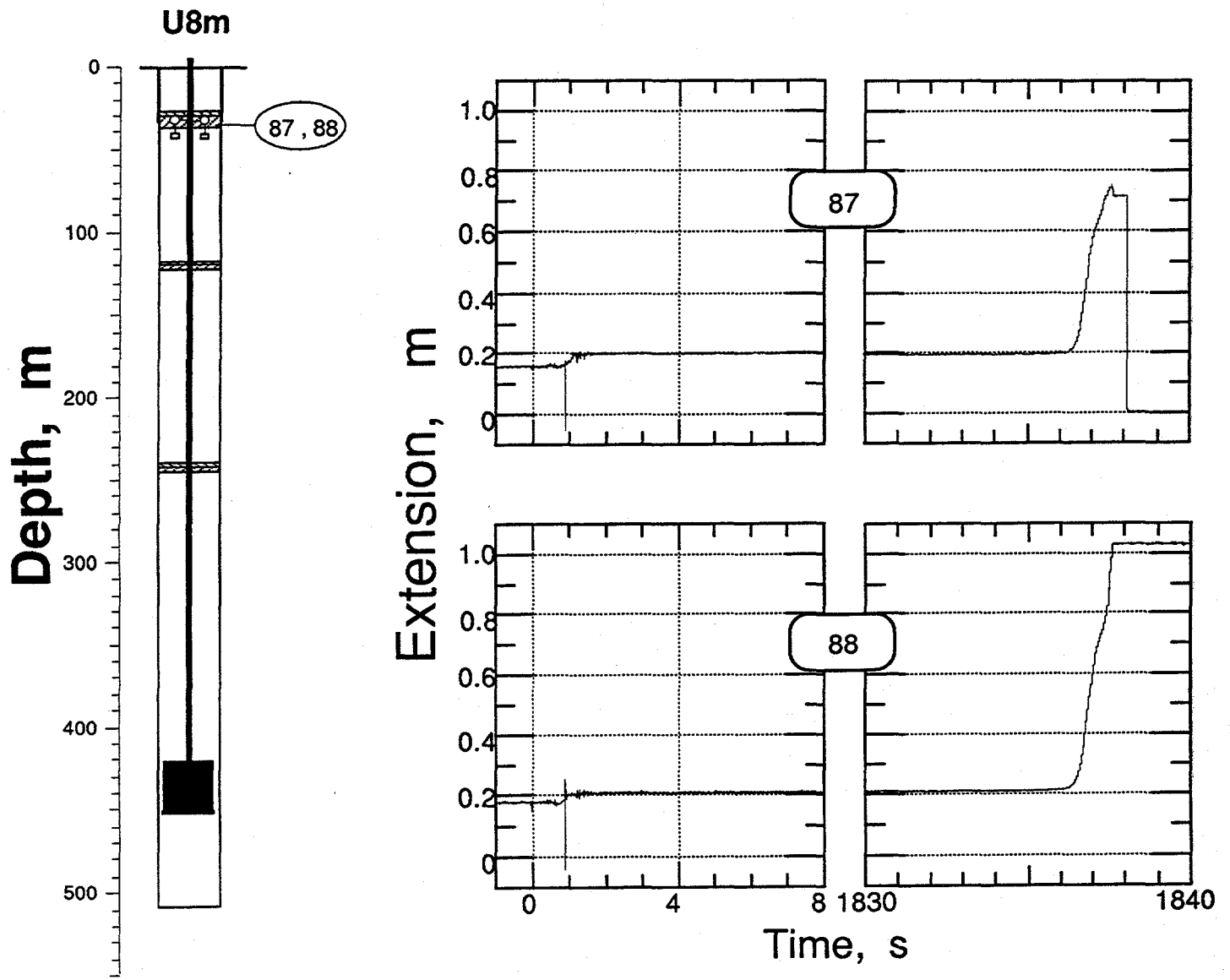


Figure 2.11 Extensometer readings from stations 87 and 88, mounted between top plug and underlying stemming.

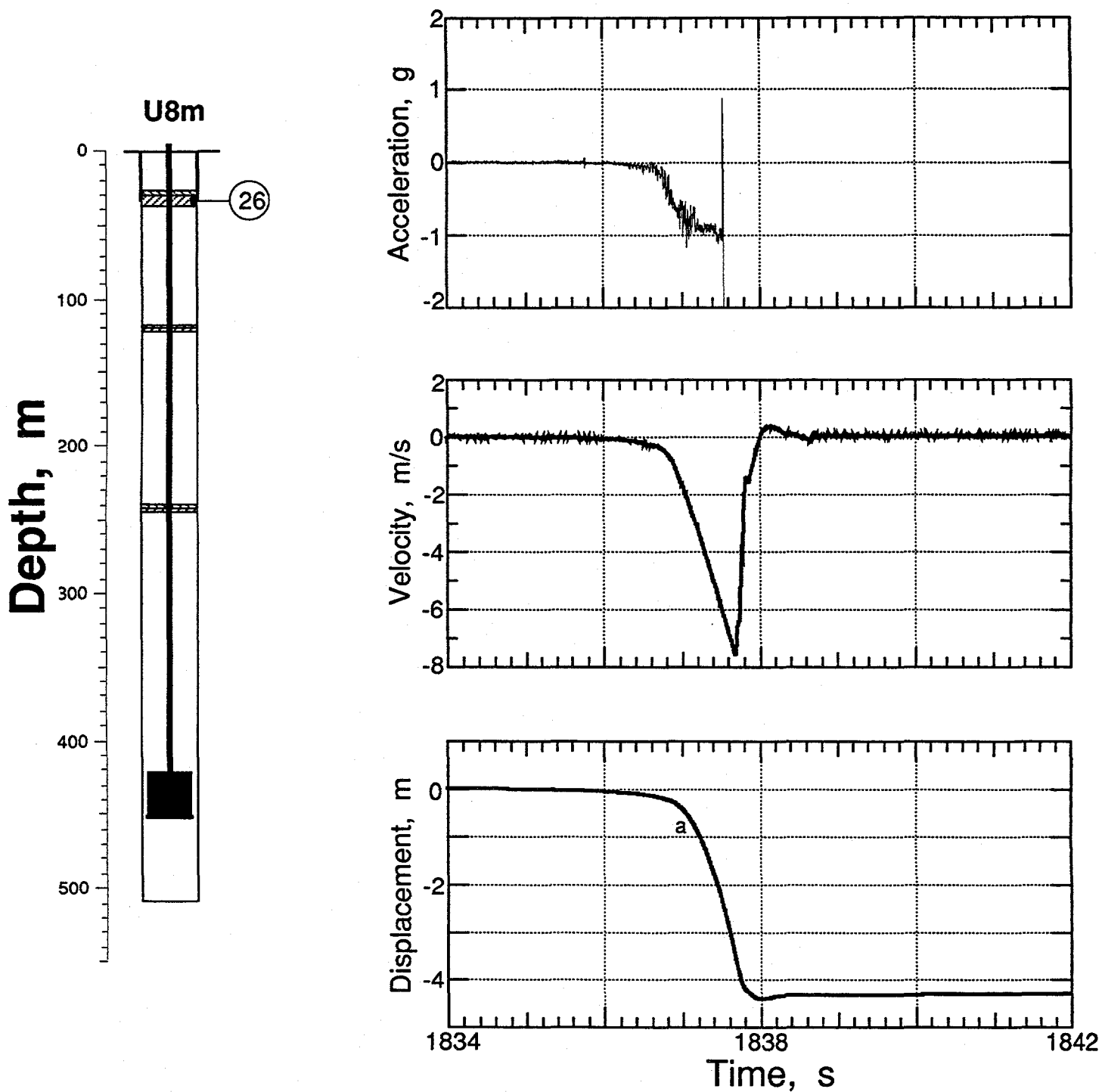


Figure 2.12 Collapse-induced vertical motion of the top plug (station 26 at a depth of 34.5 m). The traces annotated with "a" are derived from the acceleration while the velocimeter-derived signals are shown as heavy traces.

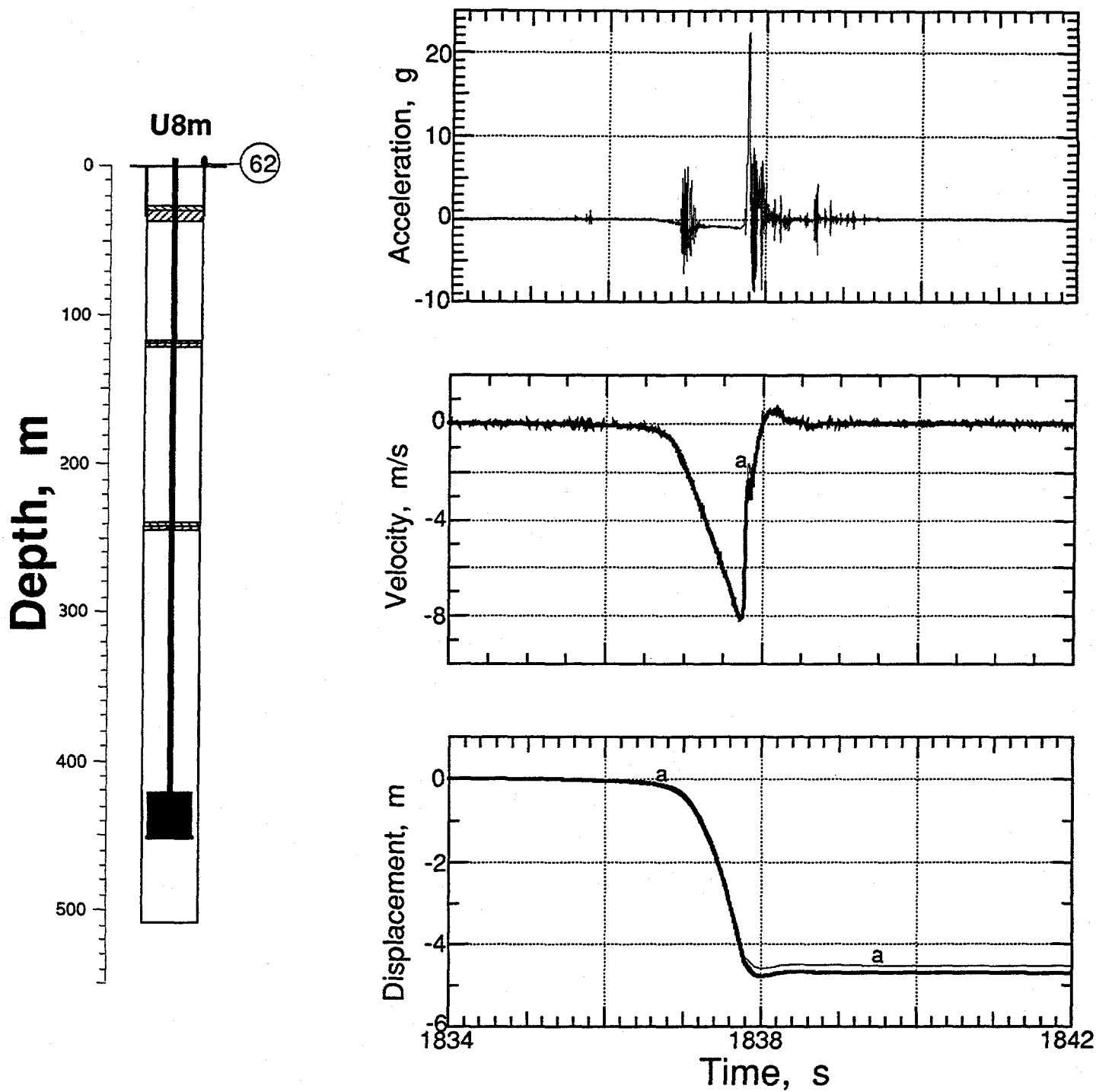


Figure 2.13 Collapse-induced vertical motion of the surface casing (station 62) The traces annotated with "a" are derived from the acceleration while the velocimeter-derived signals are shown as heavy traces.

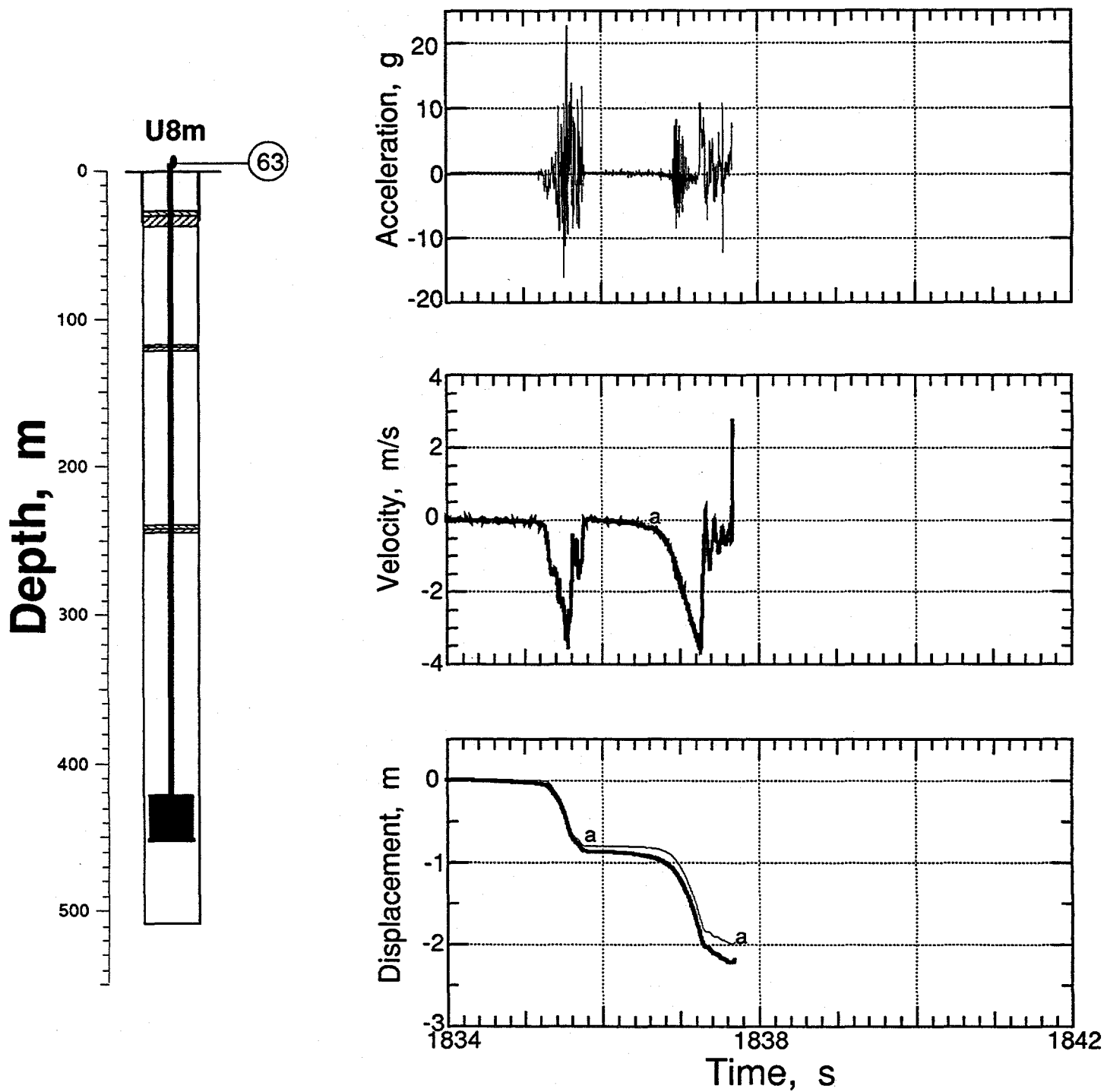


Figure 2.14 Collapse-induced vertical motion of the emplacement pipe (station 63) The traces annotated with "a" are derived from the acceleration while the velocimeter-derived signals are shown as heavy traces.

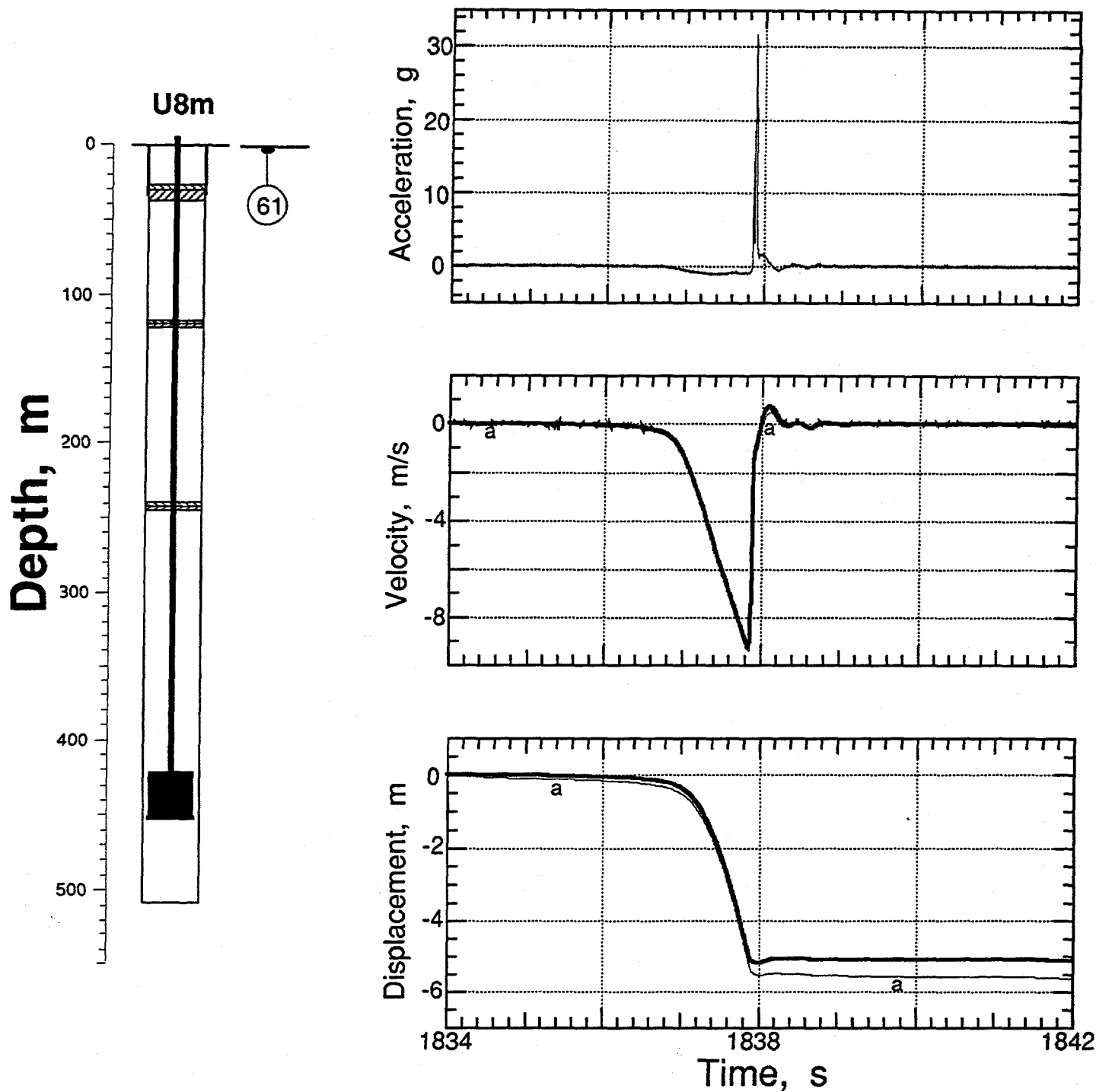


Figure 2.15 Collapse-induced vertical motion of the ground surface, 15.24 from SGZ (station 61 at a depth of 0.9 m) The traces annotated with "a" are derived from the acceleration while the velocimeter-derived signals are shown as heavy traces.

Table 2.2 Summary of Containment-Related Motion

Gauge	Slant Range (m)	Arrival Time (ms)	Acceleration Peak (g)	Velocity Peak (m/s)	Displacement Peak (cm)	Displacement Residual (cm)
26av	417.5	110(a), 219	0.96, (b), 1.66	1.05	33.5	3.5
26uv	417.5	110(a), 220	-	1.04	32.0	1.8
61av	451.4	242	1.50, 16(b)	1.20	34.2	0
61uv	451.4	245	-	1.15	31.8	-4.0
62av	452	120(a), 230	1.30, 5.2(b)	1.12	32.0	4
62uv	452	128(a), 238	-	1.13	31.2	0
63av	453.2	120(a)	(c)	6.20	129	87
63uv	453.2	122(a)	-	6.20(a), 5.9	131	90
71av	505(d)	280	1.7, 3.3(b)	1.05	18.3	0
71uv	505(d)	285	-	0.98	16.4	-3.5

(a) Pipe-induced motion.

(b) Slap-down.

(c) Signal exceeds system limits; peak only approximate.

(d) Station in recording trailer, range approximate.

Table 2.3 Containment-Related Accelerometer Characteristics

<u>Gauge</u>	<u>Natural Frequency (Hz)</u>	<u>Damping Ratio</u>	<u>System Range (g's)</u>
26av	268	0.65	6
61av	530	0.60	50
62av	270	0.65	6
63av	655	0.60	18
71av	220	0.65	10

Table 2.4 Containment-Related Velocimeter Characteristics

<u>Gauge</u>	<u>Natural Frequency (Hz)</u>	<u>Time to 0.5 Amplitude (s)</u>	<u>Calibration Temperature (°F)</u>	<u>Operate Temperature (°F)</u>	<u>System Range (m/s)</u>
26uv	3.70	7.80	72.3	102.0	10
61uv	3.92	8.75	75.4	72.6	10
62uv	3.84	8.90	72.4	80.9	10
63uv	3.74	8.45	72.6	89.1	8
71uv	4.00	20.4	73.9	64.1	2

3. Other measurements

Pressure and temperature were monitored in a PINEX line-of-sight pipe within the diagnostics canister at locations corresponding to elements of the PINEX. Wave forms of these quantities are shown, for completeness, in figure 3.1. Signals from these transducers were corrupted after 10 ms and the data are otherwise questionable.

Data from stations 64, 65, and 66 each consisting of a vertically mounted geophone and accelerometer are shown in figures 3.2 -3.4. As of this writing, the exact locations of the stations are unknown. Since all of the signals exceeded their respective system limits, they were digitized but not scaled to engineering units. These data are shown only for completeness.

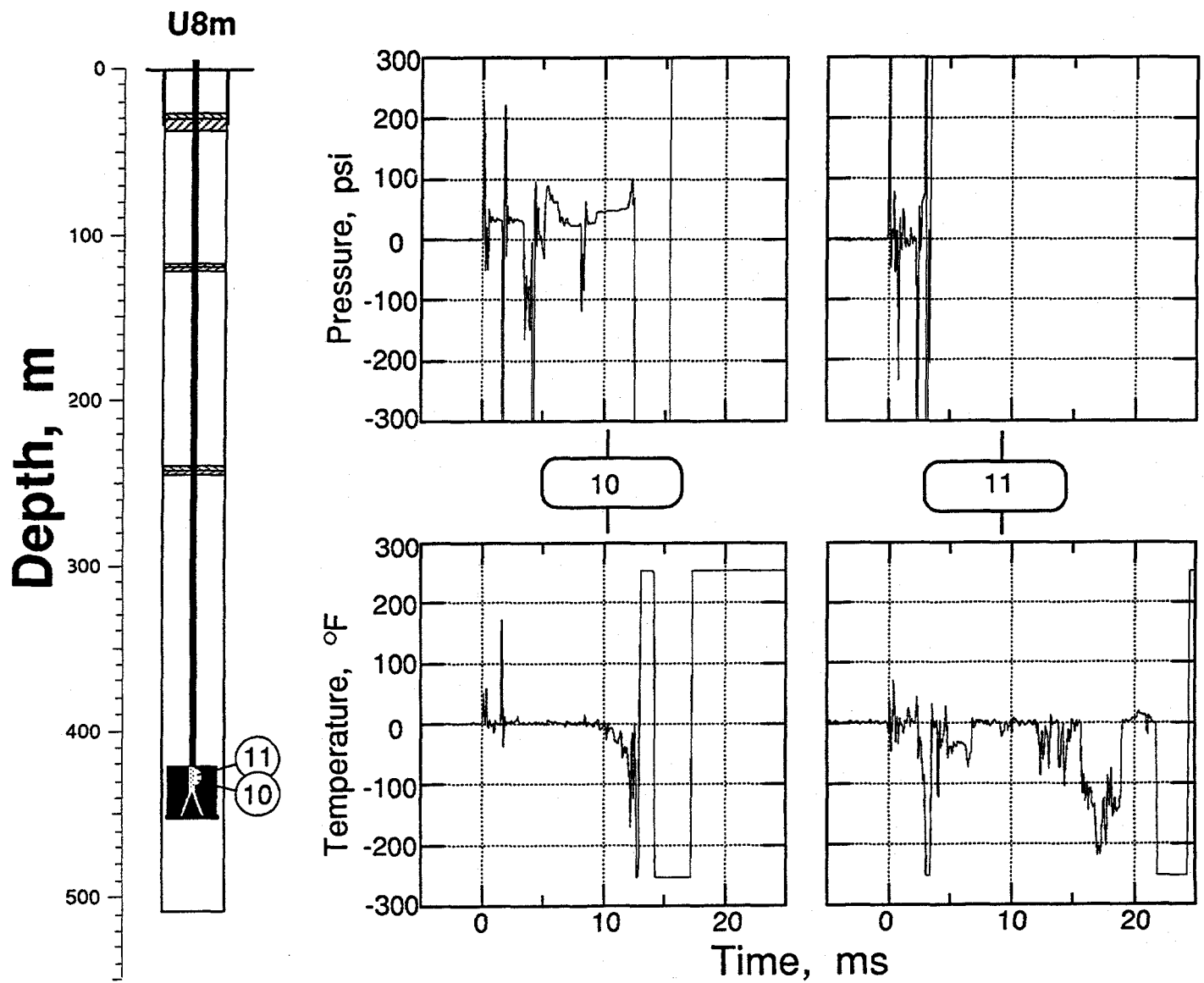


Figure 3.1 Pressure and temperature measured in a PINEX pipe. Station 10 at the elevation of the PINEX collar (20.6 m from the RD). Station 11 at the elevation of the PINEX hat (24.38 m from the RD)

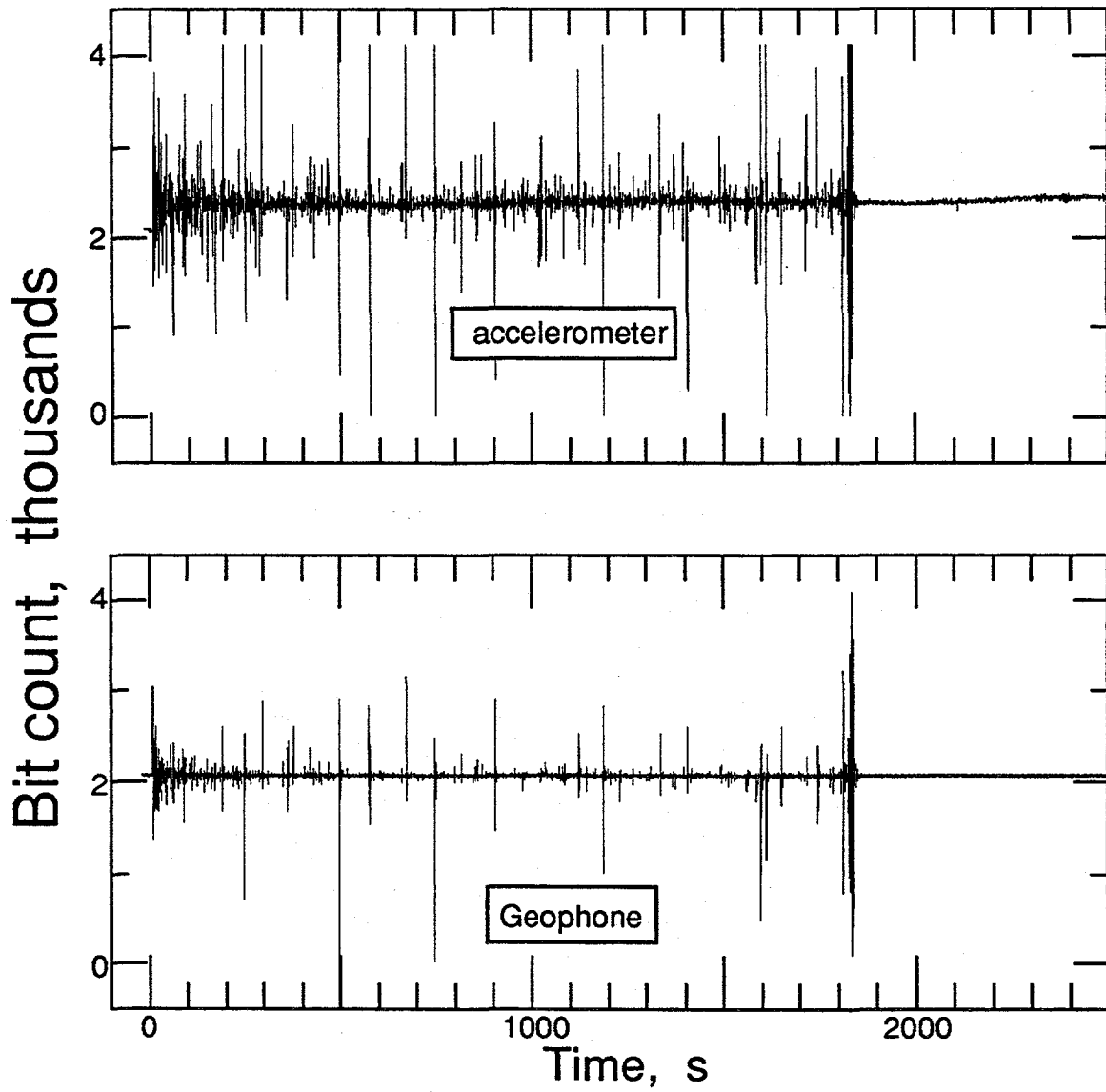


Figure 3.2 Geophone and accelerometer output from station 64. Signals are shown as digitized and the station location is unknown.

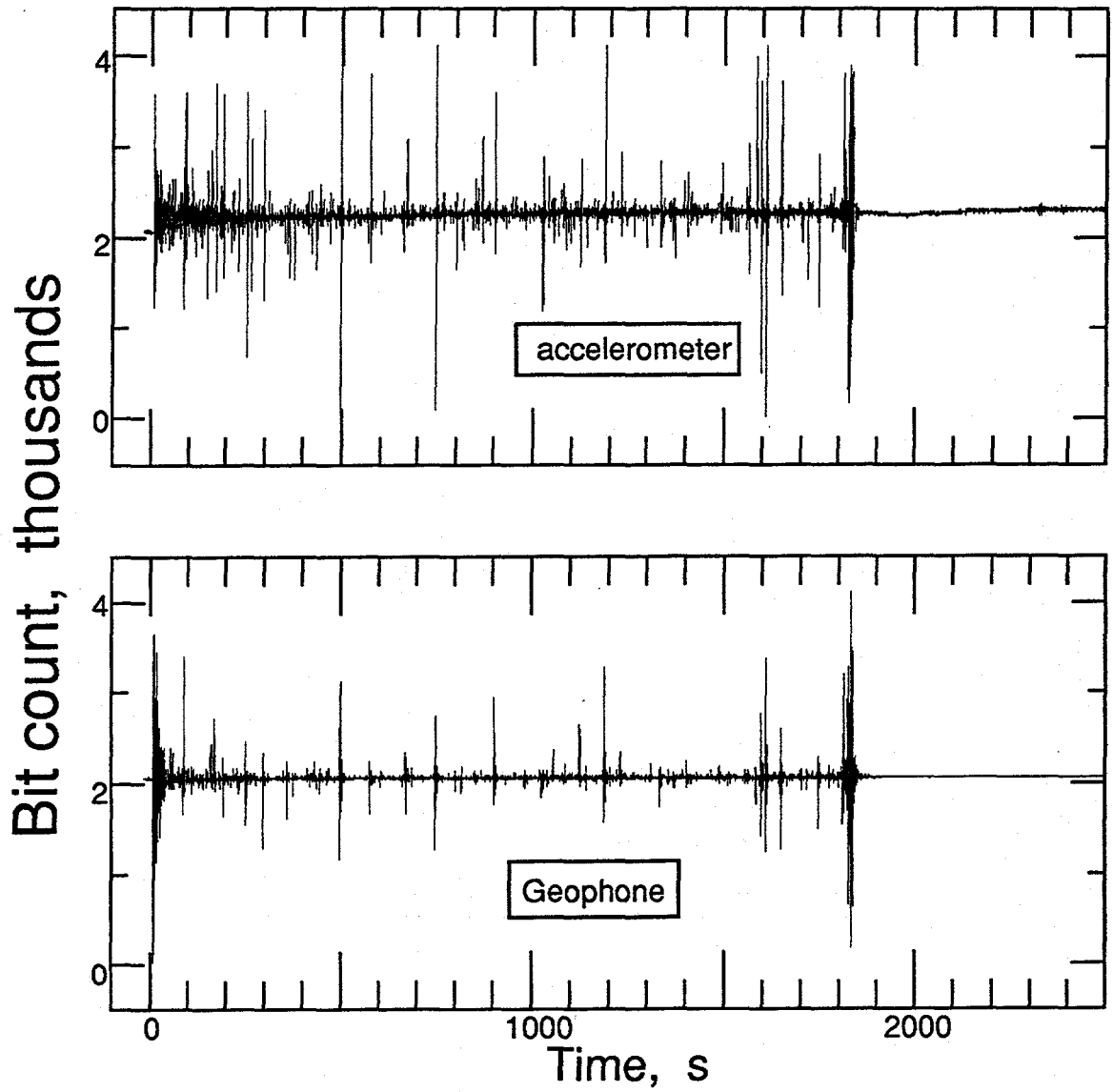


Figure 3.3 Geophone and accelerometer output from station 65. Signals are shown as digitized and the station location is unknown.

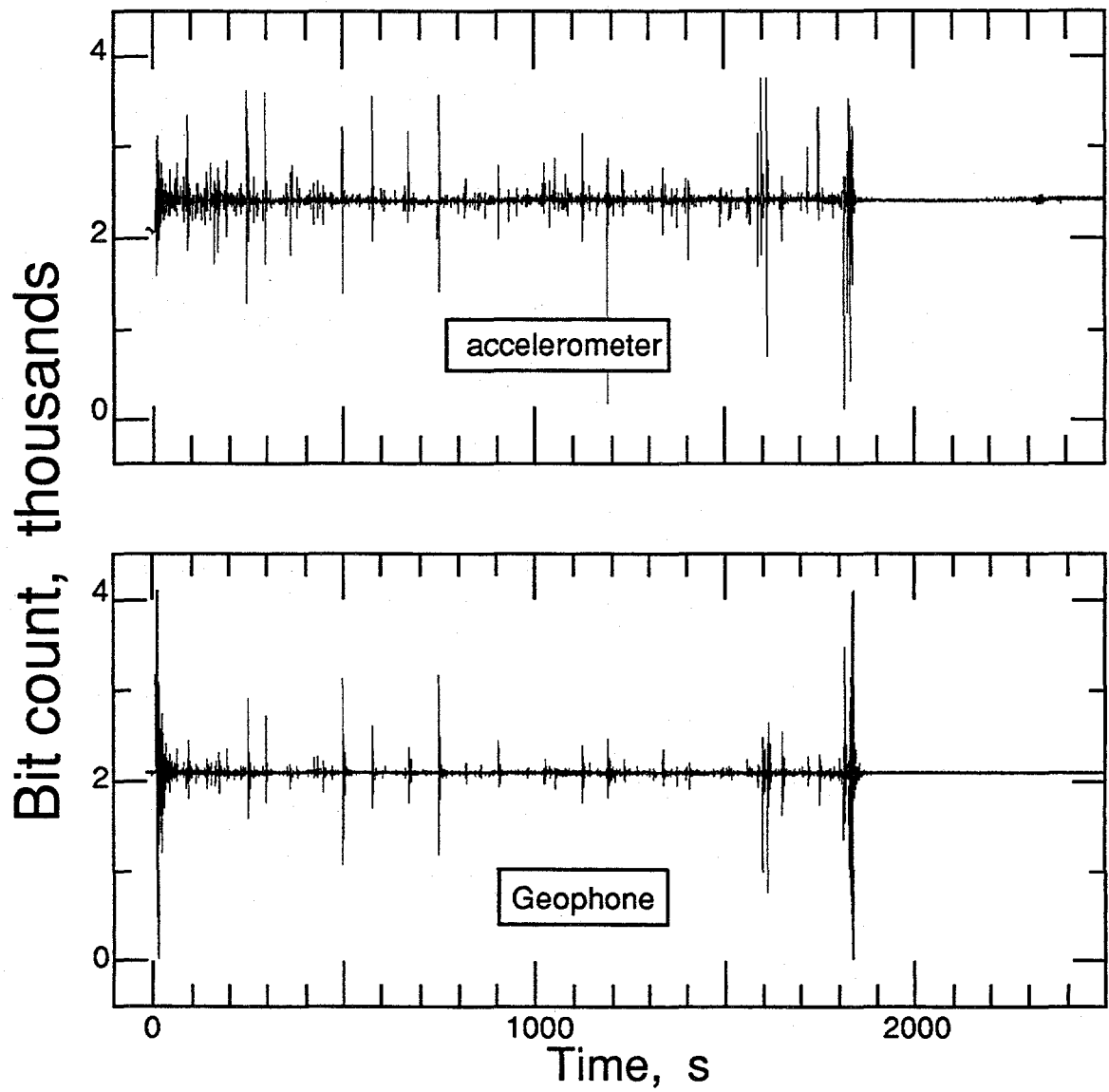
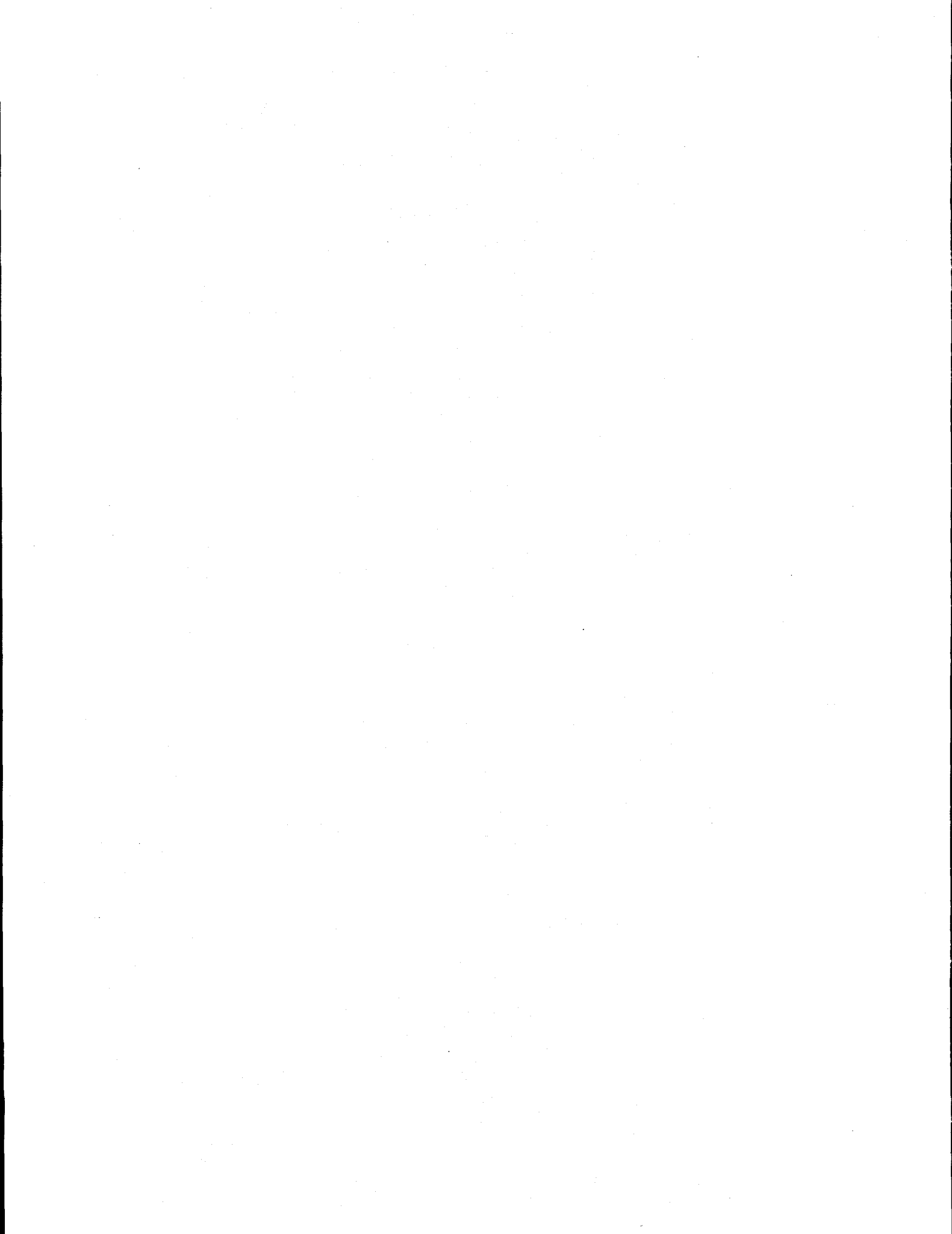


Figure 3.4 Geophone and accelerometer output from station 66. Signals are shown as digitized and the station location is unknown.

References

1. J. L. Wagoner, "U8m Preliminary Site Characteristics Summary", DM 82-32, Lawrence Livermore National Laboratory, Livermore, CA, May 11, 1982.
2. George Kronsbein, "Containment Report for U8m," Holmes & Narver, NTS:A2:82-97, September 21, 1982.
3. LLNL contacts for additional information: R. A. Heinle (CORTEX and SLIFER data)
4. Lee E. Davies, "Special Measurements Final Engineering Report FRISCO, U8m", EG&G, Energy Measurements, Las Vegas, NV, SM:82E-100-36, 1 November, 1982.
5. Lee E. Davies, "Special Measurements Physics/Instrumentation Package for FRISCO, U8m, , Revision 'A' ", EG&G, Energy Measurements, Las Vegas, NV, SM:82E-100-38, 18 November, 1982.



Distribution:

LLNL

TID (11)	L-053
Test Program Library	L-045
Containment Vault	L-221
Burkhard, N.	L-221
Cooper, W.	L-049
Denny, M.	L-205
Goldwire, H.	L-221
Hannon, W. J.	L-205
Heinle, R. (5)	L-221
Mara, G.	L-049
Moran, M. T.	L-777
Moss, W.	L-200
Patton, H.	L-205
Pawloski, G.	L-221
Rambo, J.	L-200
Roland, K.	L-221
Roth, B.	L-049
Valk, T.	L-154

LANL

App, F.	F-659
Brunish, W.	F-659
Kunkle, T.	F-665
Trent, B.	F-664

Sandia

Bergstresser, T.	MS-1159
------------------	---------

BNL/AVO

Brown, T.	A-5
Hatch, M.	A-5
Still, G.	A-5
Stubbs, T.	A-5

BNL/NVO

Bellow, B.	N 13-20
Davies, L.	N 13-20
Moeller, A.	N 13-20
Robinson, R.	N 13-20
Webb, W.	N 13-20

DNA

Ristvet, B.

S-Cubed

Peterson, E.

Eastman Cherrington Environment
1640 Old Pecos Trail, Suite H
Santa Fe, NM 87504

Keller, C.

